land

MDPI

Article

Distribution Dynamics of Park Green Spaces in China and Their Influencing Factors: Evidence from 1760 County Seats

Biao Zhang [1,2,*], Jie Xu [3,*] and Sidong Zhao [3]

[1] Visual Image Research Base of Chinese Nation, Southeast University, Nanjing 210096, China
[2] School of Design Science & Art, Nanjing University of Science and Technology, Nanjing 210094, China
[3] School of Natural Resources and Surveying, Nanning Normal University, Nanning 530001, China; sdzhao2024@nnnu.edu.cn
* Correspondence: 103200106@seu.edu.cn (B.Z.); huikit@nnnu.edu.cn (J.X.)

Abstract

Urban park green spaces are key infrastructure for improving the quality of the living environment, enhancing residents' well-being, and strengthening ecological resilience. Targeting 1760 county seats in China, this study combines the stock and incremental synergy analysis matrix, exploratory spatial data analysis, and explainable machine learning (EML) methods (SHAP) to systematically reveal the spatiotemporal patterns, spatial association characteristics, and nonlinear paths of influencing factors regarding the spatial configuration of park green spaces in county seats from 2015 to 2024. The low-stock expansion zone is dominant and concentrated in the western region and non-core urban agglomerations. The high-stock expansion zone is of the dominant type, concentrated in the eastern coastal areas and core urban agglomerations. The low-stock contraction zone and high-stock contraction zone are, respectively, marginalized lock-in and degradation risk types, requiring priority intervention. The dynamics of the park green space configuration, including the stock, increment, and their synergy, all exhibit significant positive spatial autocorrelation. The influences of the nine factors exhibit four major characteristics: directional mixing, intensity gradation, path nonlinearity, and regional heterogeneity. The threshold effect is widespread, and the inflection point value varies depending on the factor and region type. This study constructs a nonlinear and interpretable analytical paradigm and, based on empirical results, proposes a new governance framework of "zoning–grading–staging–synergy". It provides large-sample empirical evidence and theoretical support for the transformation of small-town park green spaces from "sectoral management" to "spatial governance", offering significant policy value toward achieving the precise distribution and equitable sharing of regional green space resources.

Keywords: park and green space; land resource distribution; influencing factors; county seats; China

Check for updates

Academic Editor: Xuesong Kong

Received: 6 July 2026
Revised: 12 August 2026
Accepted: 14 August 2026
Published: 19 August 2026

Copyright: © 2026 by the authors. Licensee MDPI, Basel, Switzerland. This article is an open access article distributed under the terms and conditions of the Creative Commons Attribution (CC BY) license.

1. Introduction

Green spaces are a vital component of urban ecosystems, playing an irreplaceable role in improving the quality of the human settlement environment, enhancing residents' physical and mental health, and mitigating the urban heat island effect. They represent a key pathway for implementing the United Nations Sustainable Development Goals (SDG 3, SDG 11, SDG 15) [1]. Park green spaces, as the core component of urban green space planning, are not only the main places for residents' daily leisure and recreation but also key

indicators for measuring the livability and ecological resilience of a city [2,3]. As the pace of global urbanization accelerates, the question of how to maximize both ecological benefits and social equity through the scientific distribution of park and green space resources has become a topic of great concern to governments around the world.

Countries generally incorporate spatial distribution, quality improvement, and equitable access to parks and green spaces into their spatial planning and urban governance systems [4,5]. In China, as urbanization enters its latter stage, residents' demand for high-quality recreational ecological spaces continues to rise. The rationality of the spatial distribution of park green spaces directly affects the equity and livability of urban spatial resource distribution. At present, the logic of urban development in China is shifting from "incremental expansion" to "stock quality improvement", and the spatial planning and management of park green spaces have been elevated to a national strategic level. In May 2026, the State Council issued the 15th Five-Year Plan for Urban Renewal (Guo Fa [2026] No. 12), which explicitly designates the improvement of urban green space systems and the promotion of open sharing of park green spaces as core tasks, and it sets the mandatory target of "renovating and upgrading 20,000 hectares of urban park green spaces by 2030". This policy orientation signifies that the construction of park green spaces is no longer merely an embellishment to the urban appearance or landscape but rather a hard constraint for measuring whether a city can achieve green and low-carbon transformation and improve people's well-being.

Existing research on the spatial distribution of park green spaces exhibits a significant "big-city preference", forming a pattern consisting of "big cities as the center and county seats marginalized". Case studies focusing on a specific large or megacity are the most common type found in the existing literature. Alfarhood [6], Cissé [7], Korah [8], Gül [9], and Ayele [10] applied satellite imagery and machine learning methods to systematically assess green spaces in Riyadh (Saudi Arabia), Dakar (Senegal), Kumasi (Ghana), Isparta (Turkey), and Addis Ababa (Ethiopia), including their extent, quality, pattern, accessibility, and inequality. Huang [11], Qin [12], Kukulska-Koziel [13], and Faka [14] conducted pioneering work by applying indicators such as the green space ratio, green space exposure, and the Gini coefficient. They conducted empirical analyses on 140, 368, 27, and 26 cities in China, revealing the characteristics of urban green space distribution and its influencing factors. In contrast, systematic research on park green spaces in county seats is extremely limited. Although a few studies have mentioned county seats, their focus is not on the dynamics of the park green space spatial configuration. For example, Yuan [15], Pan [16], and Shackleton [17] carried out case analyses of China and South Africa, but they did not focus on the spatiotemporal dynamics of park green space distribution. County seats differ significantly from large cities in terms of administrative hierarchy, population size, financial investment, resource endowment, land use conditions, and development stage, and the spatial configuration logic and influencing factors regarding their park green spaces may exhibit unique patterns. While these single-case studies on large or megacities have advantages in terms of data precision and methodological depth, their conclusions are highly dependent on the specific socioeconomic and geographical contexts of the studied cities. Their conclusions cannot be directly extrapolated to small-town settings or national scales.

Stock and increment are treated in isolation, failing to align with the policy orientation of land supply management. Stock research focuses on the distribution pattern, accessibility, equity, and influencing factors of urban park green spaces [18], emphasizing the evaluation of green space utilization efficiency or comprehensive benefits from the perspectives of input and output. Ajmi [19], Roslin [20], and Agustiyara [21] mapped urban green spaces in Tunisia, Malaysia, and Indonesia and assessed their distribution and

equity characteristics. Kifayatullah [22] found that the distribution of urban green spaces in Pakistan exhibits significant spatial heterogeneity and proposed sustainable management strategies. Zhao [23] established a green space multifunctional evaluation indicator system and quantitatively measured the comprehensive benefits of green spaces and their spatial heterogeneity across 285 cities in China. Wu [24] and Peng [25] shifted their focus to evaluating the efficiency of green space utilization. Incremental research focuses on revealing trends or dynamics in the increase or decrease in the number of park green spaces. Misty [26], Bizuayehu [27], and Fikri [28] analyzed and evaluated the dynamics and key driving forces of urban green spaces in Bangladesh and Ethiopia. De Lima [29] and Jia [30] analyzed the characteristics of green space degradation caused by urban sprawl in the metropolitan areas of São Paulo, Mexico City, and Shanghai and identified key influencing factors along with their marginal effects. It is noteworthy that existing research rarely incorporates both the stock of green space (existing green space) and its increment (newly added green space) into a unified analytical framework. Although a few studies have mentioned the concepts of "stock" and "increment", they generally isolate the two and mostly remain at the level of policy discussion. The Proposal of the Central Committee of the Communist Party of China on Formulating the 15th Five-Year Plan for National Economic and Social Development explicitly calls for "coordinating the comprehensive land supply of both stock and increment". The research paradigm that separates increment from stock lacks the capability for collaborative classification and integrated diagnosis in a dynamic matrix format. Therefore, it cannot effectively respond to the policy practice requirement of "coordinating the comprehensive land supply of both stock and increment", making it difficult to provide sufficient decision-making support for the scientific planning of park green spaces in the context of urban renewal.

In the field of research on the configuration and utilization of park green spaces and their influencing factors, scholars have commonly adopted classical statistics and linear spatial econometric models [31]. Zhang [32] used kernel density and network analysis methods, Moussa [33] conducted a questionnaire survey on 390 households, Wang [34] used spatial Durbin model testing, Liu [35] and Ji [36] used geographically weighted regression (GWR) techniques, and Zang [37] and Ouyang [38] further expanded to multiscale and spatiotemporal geographically weighted regression models. The strength of these methods lies in their interpretable parameters and standard statistical inference, with the underlying assumptions that relationships between variables are approximately linear, effects are additive, and there are no complex thresholds or interaction structures. This deviates from the objective mechanisms observed in reality, where economic, demographic, and policy factors are subject to threshold constraints. In recent years, some scholars have introduced machine learning models and tried to analyze the complex mechanisms of park green space distribution in reality, such as the "threshold effect", "saturation effect", and "synergy/substitution effect". Wang [39] analyzed the impacts of factors such as the population size and housing prices on the accessibility and inequality of urban parks in 314 prefecture-level cities in China using machine learning models. Cai [40] integrated different methods including ESDA, machine learning, and geographically weighted regression models and conducted a quantitative analysis of the evolution patterns and influencing mechanisms of green spaces in cities along the Grand Canal of China. These nonlinear empirical studies employing machine learning models are groundbreaking, but they all focus on large cities. There remains an insufficient understanding and empirical testing of the nonlinear mechanisms underlying the dynamic distribution of park green spaces in county seats.

Although clear guidelines have been established at the national policy level, the spatial distribution of park green spaces in county seats still faces numerous challenges in practice. Existing research has long focused on the utilization efficiency and equity of park green spaces in mega- or super-large cities or prefecture-level cities, while paying insufficient attention to the large number of county seats. In this context, systematically ascertaining the spatial configuration status and change trends of park green spaces, and scientifically revealing their influencing factors and obstacle factors, has become a key prerequisite for precisely implementing urban renewal policies and achieving the scientific planning and refined management of urban green space systems.

This study comprehensively applies technical methods such as the stock and incremental synergy analysis matrix (ISSAM), exploratory spatial data analysis (ESDA), and explainable machine learning (SHAP), targeting 1760 county seats, to systematically reveal the spatiotemporal dynamics and nonlinear formation path of the spatial configuration of park green spaces in county seats. The findings will provide a scientific basis for decision-making regarding the planning of urban green spaces and the development of park cities. To achieve the above objectives, this study focuses on the following three progressive core questions.

The first is the issue of the dynamic configuration. Specifically, which characteristics are exhibited by the temporal change trajectory and spatial distribution status of park green space supply in county seats?

The second is the issue of the path underlying nonlinear effects. Specifically, how can we understand and analyze the nonlinear path underlying the dynamic formation of the spatial distribution of park green spaces in county seats? For example, which factors have robust global significance for the dynamics of park green space distribution in county seats? Do factors such as economy, population, nature, and policy intervention have threshold effects or saturation effects? Which factors may exhibit a reversal in direction or a change in intensity across different regions and stages of development?

The third is the issue of inspiring the strategy of application transformation. Corresponding to the policy orientation of "coordinating stock and increment" in urban renewal, what targeted strategic insights can the analysis of the dynamics of park green space distribution in county seats and its influencing factors provide for urban green space planning, stock renewal, and park city development planning? How can we formulate differentiated planning intervention strategies based on the stock–increment distribution types of county seat park green spaces? How can we transform the conclusions of nonlinear path analysis into actionable policy targets?

2. Materials and Methods

2.1. Study Area

The research area covers 1760 county seats, accounting for 94.17% of the total number in China, and is highly representative. A total of 109 county seats were excluded from the study area, including all county seats in Tibet and Panshan, Tieling, Xinjin, Danba, Shiqu, Yanyuan, Zhuoni, Diebu, Xiahe, Maqin, Gande, Dari, Haimen, Longhai, Penglai, Yanshi, Fuyu, and Xinghua, due to incomplete data (Figure 1).



Figure 1. Geographical scope of the study area.

2.2. Research Methods

2.2.1. Stock and Incremental Synergy Analysis Matrix: ISSAM

In response to the policy orientation of "coordinating the comprehensive land supply of both stock and increment", this study constructs a synergistic analysis matrix of increment and stock, aiming to systematically identify the configuration dynamics of park green spaces in 1760 county seats in China, thereby achieving the scientific regulation and precise governance of small-town park green space resource distribution at the national scale. The unique value of this matrix lies in its transformation of policy principles into actionable analytical tools, achieving a transition from "describing changes" to "diagnosing types". Its advantages are evident in three areas. First, it overcomes the limitations of "looking at volume in isolation" or "looking at changes in isolation" by coupling the relative position of existing holdings with the direction of new capital inflows for a comprehensive analysis, thereby revealing asset distribution patterns rather than merely describing trends. Second, the dual-origin design combines standardization with practicality. The mean origin reflects the relative status of the region, while the zero origin directly anchors the policy judgment threshold of "expansion/degradation". Third, the four-quadrant classification results directly interface with differentiated policy design, enabling academic analysis outcomes to be smoothly transformed into the language of planning and management decisions. This transformation effectively bridges the gap between empirical research and policy practice.

The steps are as follows.

Step 1: Calculate the stock index using Equation (1) [41]. First, identify the maximum value of the park green space area among the 1760 county seats during the study period. Then, use the ratio of each county's park green space area to this maximum value as a

relative share index to eliminate the interference of scale differences between county seats in the judgment of existing stock.

$$SI = \frac{Y_i}{Y_{j-max}} \times 100\% \quad (1)$$

$$II = \left(\sqrt[t]{\frac{Y_{i-end}}{Y_{i-base}}} - 1 \right) \times 100\% \quad (2)$$

where SI: stock index of park green space distribution; II: incremental index of park green space distribution; PGS_i: the scale of park green space distribution in county i; PGS_{j-max}: the maximum scale of park green space distribution among all county seats in year j; Y_{i-base}: the scale of park green space distribution in county seat i in 2015; Y_{i-end}: the scale of park green space distribution in county seat i in 2024.

Step 2: Calculate the incremental index using Equation (2) [42]. The average annual growth rate of the park and green space area in 1760 county seats from 2015 to 2024 is calculated to reflect long-term trends in increases and decreases.

Step 3: Establish a coordinate system. A two-dimensional analysis plane is established with the relative share index as the abscissa (representing the stock level) and the average annual growth rate as the ordinate (representing the incremental trend).

Step 4: Determine the origin of the horizontal axis and set the threshold for stock analysis. The average value of the stock indices of all 1760 county seats is taken as the origin of the horizontal axis to reflect the regional status of each county seat within the study area. Areas with values above the mean are classified as "areas with high stock and a competitive advantage", while those below the mean are classified as "areas with low stock and a competitive disadvantage".

Step 5: Determine the origin of the y-axis and set the threshold for incremental analysis. Ultimately, both policy requirements and public demand call for the distribution of more parkland and green spaces to improve the quality of the living environment in each county seat. In reality, park green spaces are sensitive and prone to encroachment and compression by residential, industrial, commercial, and other land uses, and the reduction or degradation of green spaces is a prevalent phenomenon [43]. Therefore, zero is chosen as the threshold to strictly define the two evolutionary states: "expansive" and "regressive".

Step 6: Divide the data into four quadrants to establish clear guidelines for zone-based management. The 1760 county seats are divided into four categories, providing a targeted basis for the design of zoned and differentiated green space management policies. The high-stock expansion zone is considered an ideal model; in the future, efforts should be made to obtain certifications such as "Garden City" and "Forest City" and build regional demonstrations. The high-stock contraction zone is classified as being at risk of degradation. In the future, efforts should be made to conduct urban health assessments to determine the status and causes of the reduction or degradation of park green spaces and to carry out targeted urban renewal and ecological restoration. The low-stock expansion zone is classified as an area requiring improvement. In the future, monitoring and early warning systems should be strengthened, and regular analyses should be conducted to determine whether the distribution of park green spaces aligns with the population demand and economic carrying capacity, thereby avoiding waste resulting from overdistribution. The low-stock contraction zone is classified as a marginalized and locked-in type and represents an area where future policies should prioritize intervention. It requires the simultaneous implementation of strategies to expand park and green spaces and revitalize existing resources, taking into account the needs of the permanent resident population, the local economy's carrying capacity, and the availability of external support [44,45] (Figure 2).

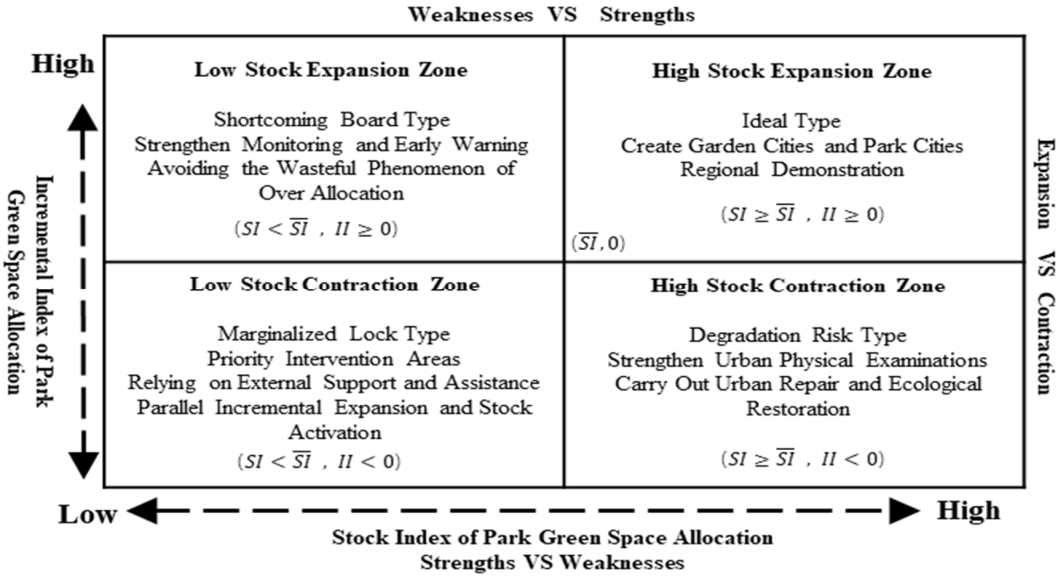


Figure 2. Schematic diagram of stock and incremental synergy analysis matrix.

2.2.2. Exploratory Spatial Data Analysis: ESDA

This study covers 1760 county seats nationwide, and the configuration of park green spaces in these county seats is not randomly distributed, potentially exhibiting significant spatial dependence or spatial heterogeneity. If this spatial effect is ignored, traditional statistical methods will struggle to accurately capture the true spatial structure of park and green space distribution. ESDA quantifies the degree of spatial dependence through statistical measures and visually reveals spatial heterogeneity, enabling researchers to quickly identify "polarized" areas and outliers in the green space configuration [46].

By incorporating ESDA into the study of green space distribution in small-town parks, this study accurately identifies the geospatial distribution patterns and autocorrelation characteristics of 1760 county seat-level park green spaces based on the data. On the one hand, the global Moran's I test is used to determine whether the stock and incremental distributions of park green spaces in the 1760 county seats exhibit significant spatial autocorrelation overall. An index value greater than zero indicates a positive correlation, meaning that county seats with high or low values tend to be located near one another. An index value less than zero indicates a negative correlation, meaning that high and low values are spatially intermixed. An index value equal to or close to zero indicates that the distribution tends toward a random distribution. On the other hand, by visualizing the distribution of county seats through local Moran's I (LISA) clustering maps, this study accurately identifies the four types of spatial association—HH, LL, HL, and LH—and intuitively illustrates the spatial structure of "high-distribution" and "low-distribution" areas for park green spaces, thereby providing a spatial foundation for the further analysis of the influencing factors. In addition, this study uses the Gini coefficient to measure the degree of spatial heterogeneity in park green space distribution in county seats and employs spatial clustering methods to conduct a visual analysis. The calculation equations for the global and local Moran's I index [47] and Gini coefficient [48] are as follows:

$$\text{Global Moran's } I_i = \frac{n}{S_0} \times \frac{\sum_{i=1}^{n}\sum_{j=1}^{n} W_{ij}(D_i - \overline{D})(D_j - \overline{D})}{\sum_{i=1}^{n}(D_i - \overline{D})^2} \quad (3)$$

$$\text{Local Moran's } I_i = Z_i \sum_{i=1}^{n} W_{ij} Z_j \quad (4)$$

$$S_0 = \sum_{i=1}^{n} \sum_{j=1}^{n} = W_{ij} \tag{5}$$

$$G_i = \frac{\sum_{i=1}^{n} \sum_{j=1}^{n} |D_i - D_j|}{2n^2\mu} \tag{6}$$

where n is the number of county seats in the study area (1760); D_i and D_j are, respectively, variable values for county seats i and j, where $\overline{D}$ is their mean; W_{ij} represents the spatial weight matrix in global spatial autocorrelation and the row-standardized value of spatial weights in local spatial autocorrelation; S_0 is the sum of the spatial weight matrix; Z_i and Z_j are standardized values for county seats i and j; and μ is the mean of the data in the study area. The spatial weighting uses a queen adjacency matrix, with a maximum number of neighbors of 14 and an average number of neighbors of 4.69.

2.2.3. Explainable Machine Learning: EML

SHAP, based on the Shapley value in cooperative game theory, achieves the fair attribution of feature influence by calculating the marginal contribution of each feature to the model prediction across all possible combinations of feature subsets [49]. The core advantage lies in additive consistency, ensuring the integrity and interpretability of attribution [50]. SHAP is independent of specific model types and can be used in conjunction with mainstream machine learning models such as XGBoost, LightGBM, and RandomForest. With the advancement of urban renewal, the spatial configuration of park green spaces in county seats is influenced by the interplay of multidimensional factors, including the natural background, economic development, population structure, and policy interventions. Complex nonlinear and interactive effects exist among these influencing factors. Traditional linear regression models (such as OLS and GWR) have difficulty in capturing the threshold effects and inflection point characteristics among variables; thus, they are likely to result in misinterpretations of the underlying path. Therefore, the introduction of the SHAP algorithm—a method for EML—is an inevitable choice for accurately analyzing the complex influencing factors behind green space distribution in county seats [51].

The analysis steps using EML in this study are as follows.

Step 1: Conduct data preprocessing and model training. To enhance the robustness and reliability of the model, this study uses three models—RandomForest, LightGBM, and CatBoost—for simultaneous training. The dataset is partitioned for training under multiple schemes with proportions of 60%, 70%, 80%, and 90%, and the result with the best performance is selected for analysis. A SHAP value is assigned to each feature of each data point to quantitatively describe how this feature affects the prediction result in the process of model construction. Each predicted value must satisfy Equation (7). Moreover, for each feature, Equation (8) is used to calculate the mean of the absolute values of its global SHAP values, so as to compare the importance of features.

$$Y_m = Y_{base} + f(X_{m1}) + f(X_{m2}) + \ldots + f(X_{mh}) \tag{7}$$

$$\overline{C_h} = \frac{1}{n} \sum_{m=1}^{n} |f(X_{mh})| \tag{8}$$

where m is the number of machine learning samples; n is the total sample size; h is the specific feature of the m-th sample; Y_{base} is the baseline value of the entire model—typically, the mean of the target variable across all samples; and $f(X_{mh})$ is the SHAP value of the m-th sample for the h-th feature, i.e., the contribution to the predicted value Y_m. When

$f(X_{mh}) > 0$, it indicates that this feature has a positive effect on the prediction. $\overline{C_h}$ is the mean of the absolute values of the global SHAP values for feature h.

Step 2: Analyze the direction and nature of the impact of each factor. The SHAP main effect plot is used to observe the positive and negative changes in the Shapley value, corresponding to changes in the characteristic values. It can further determine whether each factor (such as economic level, population density, and fiscal expenditure) has a positive correlation effect or a negative inhibitory effect on the distribution of park green spaces in county seats.

Step 3: Analyze the magnitude of the factor impact intensity. A SHAP feature importance plot (based on the mean absolute Shapley values of all samples) is generated to globally rank the influencing factors, thereby identifying the dominant factors that play a stable and globally significant role in the dynamics of park green space distribution across 1760 county seats. Moreover, the spatial disparities in the effects of promoting and inhibiting factors are analyzed using the Gini coefficient.

Step 4: Analyze the nonlinear paths of factor effects. The SHAP dependency graph is utilized to visually present the dynamic trajectory of the impacts of single-variable value changes on the green space configuration, accurately capturing the threshold and inflection point where the influence effect experiences "direction reversal" or "intensity transition" and revealing its nonlinear path of action.

To ensure the robustness of the data analysis results, we took the following measures. First, we trained the models using RandomForest, LightGBM, and CatBoost to rule out the possibility of unstable results caused by inappropriate model selection. The parameters are the default settings recommended by the software, with the training set ratio set to 70% and Bayesian auto-optimization selected as the optimization method. Second, we compared the Train Acc, Test Acc, Test Precision, Test Recall, and Test F1 metrics. After ruling out solutions with poor performance or overfitting, we selected RandomForest as the most effective approach. Third, we split the data into subsets (60%, 80%, and 90%) to further train and test the selected RandomForest model, thereby eliminating any instability in the results that might result from improper dataset splitting. Fourth, we conducted 10-fold cross-validation on the RandomForest model using the 70% training set. The 10 scores are 0.7419, 0.7398, 0.7724, 0.7236, 0.7642, 0.7236, 0.7805, 0.7967, 0.7480, and 0.6992, respectively. The average accuracy is 0.748990, and the ** standard deviation is 0.028209. After further comparison of the parameters, we ultimately selected the RandomForest model with 70% of the data allocated to the training set and conducted an empirical analysis of its output results (Table 1).

Table 1. Model robustness analysis.

Model	Train Acc	Test Acc	Test Precision	Test Recall	Test F1	Training Set Ratio
RandomForest	0.80	0.76	0.68	0.76	0.72	70
LightGBM	0.78	0.76	0.68	0.76	0.71	70
CatBoost	0.87	0.75	0.67	0.75	0.70	70
RandomForest	0.79	0.75	0.67	0.75	0.70	60
RandomForest	0.82	0.74	0.67	0.74	0.70	80
RandomForest	0.81	0.74	0.66	0.74	0.70	90

2.3. Indicator Selection and Data Sources

Park green space refers to green spaces in county seats that are open to the public, primarily serving recreational functions while also fulfilling roles in ecology, beautification, and disaster prevention. The data are mainly derived from the China County Seat Construction Statistical Yearbook and the China Urban Construction Statistical Yearbook. The

dependent variable is the analysis result of the ISSAM, and the text variable is directly used. Therefore, the EML analysis is performed by classification. The selection of independent variables takes into account three aspects, namely demand, supply capacity, and ecological environment conditions, with a total of 9 indicators (Table 2). Most of the data are sourced from the China Statistical Yearbook (County-Level) and the China City Statistical Yearbook. There is only one missing data point for park green space, with a total of four missing independent variable data. Some missing data are filled in with data from adjacent years. For example, park and green space data from 2024 are estimated by extrapolating trends from data from 2022 and 2023. Some of the missing data come from authoritative channels such as government statistical bulletins and official news reports—for example, the precipitation data from Changhai, Shengsi, Nan'ao, and Linxia. The proportion of missing data is extremely low, and interpolation via scientific methods or other authoritative channels has little impact on the analysis results.

Table 2. Indicator selection and data sources.

Indicator	Abbreviation	Unit	Data Source
Population density	PD	Persons	China Statistical Yearbook (County-Level) and China City Statistical Yearbook
Gross domestic product	GDP	Billions	
Rationalization index of industrial structure	RIIS	No unit	
Fiscal self-sufficiency rate	FSSR	%	
Temperature	T	Celsius	National Tibetan Plateau Data Center
Precipitation	P	Millimeters	
Particulate matter 2.5	PM2.5	Micrograms/cubic meters	
Surface undulation	SU	No unit	Institute of Geographic Sciences and Natural Resources Research, Chinese Academy of Sciences
Number of scenic spots	NSS	Pieces	POI

The main reasons for selecting these indicators are as follows.

From the demand perspective, population density (PD) represents the scale of potential green space users per unit area and is a core indicator for measuring the demand intensity of park green spaces [52]. The gross domestic product (GDP) serves as a comprehensive benchmark for measuring the level of county economic development, reflecting the overall wealth creation capacity of the region. Economically developed regions generally exhibit stronger willingness to pay and a higher consumption capacity, which can generate demand for higher-quality green spaces (e.g., specialized parks and pocket parks). Moreover, the land appreciation driven by GDP growth will further intensify land use competition, indirectly affecting the spatial distribution priority of green spaces [35].

Regarding the supply dimension, the rationalization index of the industrial structure (RIIS) represents the degree of coordination between industries and the efficiency of resource distribution [53]. Regions where the industrial structure tends to be rationalized usually have a higher proportion of tertiary industry, have a stronger demand for a livable environment, and, at the same time, exhibit relatively low pressure in terms of land use competition, which is more conducive to the continuous supply and spatial optimization of park green spaces. The fiscal self-sufficiency rate (FSSR) measures the fiscal autonomy of local governments, calculated as the ratio of local general public budget revenue to expenditure [24]. Parks and green spaces are public goods by nature, and their construction and maintenance rely heavily on government funding. A high FSSR means that the county has greater autonomous financial resources for the construction and maintenance of public

green spaces; conversely, county seats that rely on transfer payments or land finance are susceptible to macroeconomic policy fluctuations, resulting in poor stability.

From the perspective of ecological environmental conditions, hydrothermal conditions serve as the natural foundation for vegetation growth, directly impacting the cost and effectiveness of park green space construction. This study uses temperature (T) and precipitation (P) to characterize the influence of climatic conditions on the dynamics of the park green space configuration [3]. Particulate matter 2.5 (PM2.5) reflects the degree of air pollution and is also an implicit signal of residents' demand for green space ecological services [54]. Surface undulation (SU) determines land availability, construction costs, and the distribution and morphology of park green spaces [55,56]. The number of scenic spots (NSS) reflects an important tourism resource for county seats, reflecting the region's ecological quality and scenic appeal [57]. National-level or provincial-level scenic areas, nature reserves, or A-level tourist attractions will significantly alter the logic behind green space planning. NSS data are derived from POI data obtained through web crawling technology.

3. Results

3.1. Stock Feature

3.1.1. Distribution Pattern of Park Green Spaces in Base Period

In 2015, the 1760 county seats in China covered a total area of 244,559.24 hectares. The maximum value reaches 1090 hectares, with both Zhucheng and Xintai exceeding 1000 hectares. The minimum value is only 1.00 hectares, seen in areas including Baiyu, Xiangcheng, Huangping, Danzhai, Lintan, Tongde, Qumalai, and Wufeng. Regarding the data distribution, the mean is 138.95 hectares, but the median is only 101.00 hectares, indicating a severe right-skewed distribution, with the land stock in most county seats remaining at a low level. In terms of spatial differentiation, the coefficient of variation is as high as 0.93, and the Gini coefficient is 0.46—which is also above the international warning threshold of 0.4—indicating significant disparities in the size of the park green space stock among different county seats.

Using a quantile-based spatial clustering method, the stock of park green space in all 1760 county seats is classified into four tiers. Zhucheng, Xintai, Rongcheng, and Yixing are classified as higher, mostly located in the eastern coastal provinces of Shandong, Jiangsu, and Zhejiang and the municipality of Shanghai. Nenjiang, Jianping, Fukang, Linzhang, Zhangpu, Pingyuan, Mingguang, Gong'an, Huimin, and Jishou are classified as high, mostly located in the central region (Anhui, Jiangxi, Hunan, Hubei), the Chengdu–Chongqing urban agglomeration, and Guangdong. Huidong, Hanyin, Liancheng, and Youxi are classified as low, with most located in the middle reaches of the Yangtze River (especially Hubei) and the northeastern region. Yongji, Shitai, Xiajiang, and Tuoli are classified as lower, mostly located in the western region, particularly Xinjiang, Gansu, Qinghai, Yunnan, and Guizhou (Figure 3).

In 2015, the global Moran's index reached 0.45 ($Z = 26.90$, $p < 0.001$), indicating significant positive spatial autocorrelation in the distribution of park green space stock across the 1760 county seats in China. From the local spatial autocorrelation visualization analysis, HH clusters are highly concentrated in the eastern coastal regions of Shandong, Jiangsu, Zhejiang, and Shanghai, with small clusters also present in Central China, such as Jiangxi, Hubei, and Anhui, as well as Guangdong. LL is highly concentrated in the western region, particularly in Xinjiang, Gansu, Qinghai, Sichuan, Yunnan, and Guizhou. HL and LH areas are fewer in number and scattered (Figure 3).

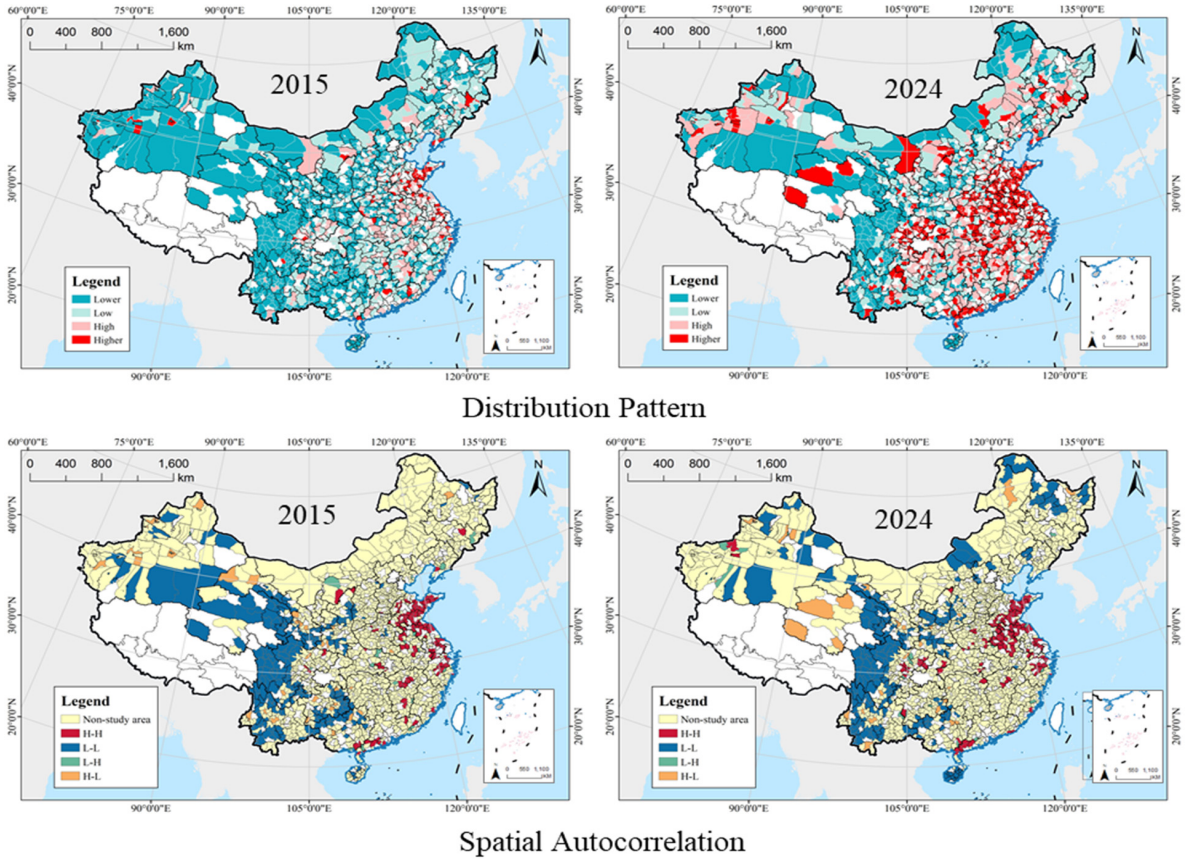


Figure 3. Distribution pattern and LISA of park green spaces in 2015 and 2024.

3.1.2. Distribution Pattern of Park Green Spaces in End Period

In 2024, the stock of park green spaces reached 370,918.84 hectares. The maximum value occurs in Yiwu, reaching 1790 hectares. Akesu, Kunshan, Zhucheng, Rongcheng, Zhuji, Anqiu, Kashi, and Yanji also exceed 1000 hectares. The smallest area is just 2.00 hectares, located in Henan. From the data distribution, the mean is 210.75 hectares and the median is 159.21 hectares, and they still exhibit a right-skewed distribution. From the perspective of spatial imbalance, the coefficient of variation is as high as 0.85, and the Gini coefficient stands at 0.42, still above the international warning line of 0.4.

The quantile spatial clustering analysis results show that Nanchang, Xingyi, and Yueqing are classified as higher. High-value areas are widely distributed across the country but are more densely concentrated in the lower reaches of the Yellow River Basin, the Yangtze River Basin, and coastal areas. Huaiji, Linwu, and Xingping are classified as high, mostly located in the middle reaches of the Yangtze River urban agglomeration, the Chengdu–Chongqing urban agglomeration, the west coast of the Taiwan Strait urban agglomeration, Northeastern China, and the border areas adjacent to Western Xinjiang. Wengyuan, Qingtian, and Debao, among others, are classified as low, with most located in the Beijing–Tianjin–Hebei metropolitan area, the northeastern border region, and the Beibu Gulf urban agglomeration. Keshan, Ningling, and others are classified as lower. They are mostly located in the western region, including Yunnan, Qinghai, Gansu, Xinjiang, and Ningxia (Figure 3).

The global Moran's index for 2024 reached 0.40 ($Z = 24.77$, $p < 0.001$), indicating that the positive spatial autocorrelation of park green space distribution has decreased but remains at a relatively high level. Based on the local spatial autocorrelation visualization analysis, the distribution pattern maintains overall stability. Changes primarily occur in localized areas, especially in the LL and HH groups. LL clusters have shrunk significantly

in the western region, especially at the junction of Xinjiang, Qinghai, Guangxi, and Guizhou. In addition, LL has experienced significant expansion in the northeastern border and the middle reaches of the Yellow River. HH has expanded significantly in the lower reaches of the Yellow River Basin (particularly in Shandong) and the upper reaches of the Yangtze River Basin (particularly in the Chengdu–Chongqing metropolitan area), while remaining largely stable in the Yangtze River Delta and the Greater Bay Area and contracting slightly in other regions (Figure 3).

3.2. Incremental Feature

3.2.1. Change Quantity of Park Green Spaces During the Research Period

Between 2015 and 2024, 1545 county seats expanded their park and green space areas, accounting for 87.78% of the total, indicating that expansion has become the dominant trend in changes to park and green space areas. From 2015 to 2024, park green spaces expanded by a cumulative total of 136,668.11 hectares, with an average of 88.46 hectares and a median of 59.00 hectares. Akesu saw the largest increase, reaching 908.24 hectares. Yiwu, Zichang, and Yanji also experienced relatively large expansions, all exceeding 500 hectares. In the east, the large-scale expansion of county seats mostly occurs in the core areas of urban agglomerations, such as the Yangtze River Delta and the Pearl River Delta. In the west, it is concentrated in national economic zones, strategic corridors, border zones, etc. The minimum expansion value was only 0.30 hectares, located in Huixian. In addition, Youyu, Wenxi, and Mulei all saw only minor increases, with none exceeding 1 hectare. These types of county seats, with marginal growth, are mostly densely distributed in areas with harsh natural conditions (such as the arid northwestern region and the high-altitude cold region of the Qinghai–Tibet Plateau) or at the junctions of provincial administrative regions. The coefficient of variation for the increment in park green spaces is 1.15, and the Gini coefficient reaches 0.53, far exceeding the international warning threshold of 0.4, indicating significant spatial heterogeneity in the expansion of park green spaces. The quantile spatial clustering analysis results show that high- and higher-class expansions are more concentrated in the middle reaches of the Yellow River Basin, the middle and upper reaches of the Yangtze River Basin, the Yunnan–Guizhou Plateau, the Beibu Gulf urban agglomeration, and the western border area of Xinjiang (Figure 4).

From 2015 to 2024, 195 county seats experienced a reduction in park green space, accounting for 11.08%, indicating that degradation cannot be ignored. During the study period, the cumulative reduction in park green space was 10,308.51 hectares, with an average of 52.86 hectares and a median of 30.30 hectares. Xingning saw the largest decrease, amounting to 549.34 hectares. Longyao, Xintai, and Wuhua also saw significant declines, all exceeding 300 hectares. During the rapid urbanization and industrialization processes in these areas, conflicts over land use, such as industrial park replacement, old city renewal, or new district expansion, have led to the temporary occupation of existing affiliated green spaces. The smallest area of land loss was just 0.20 hectares, located in Chishui. In addition, the areas of land loss in Bazhou, Xiongxian, and Henan were all relatively small, with none exceeding 1 hectare. The county seats with marginal reductions mostly belong to agricultural, semi-agricultural, and semi-pastoral areas. Their urban development intensity is low, and the annual fluctuations in parks and green spaces are mainly due to sporadic small-scale infrastructure adjustments or natural factors, without a systematic decline trend. The coefficient of variation for the reduction in park green space was 1.34, and the Gini coefficient reached 0.57; both are higher than those observed during expansion, indicating that the contraction of park green spaces exhibits more significant spatial heterogeneity. The reduction in park green spaces was entirely classified as lower, with a more concentrated

distribution in Hainan, Xinjiang, Qinghai, Inner Mongolia, and the northeastern region (Figure 4).

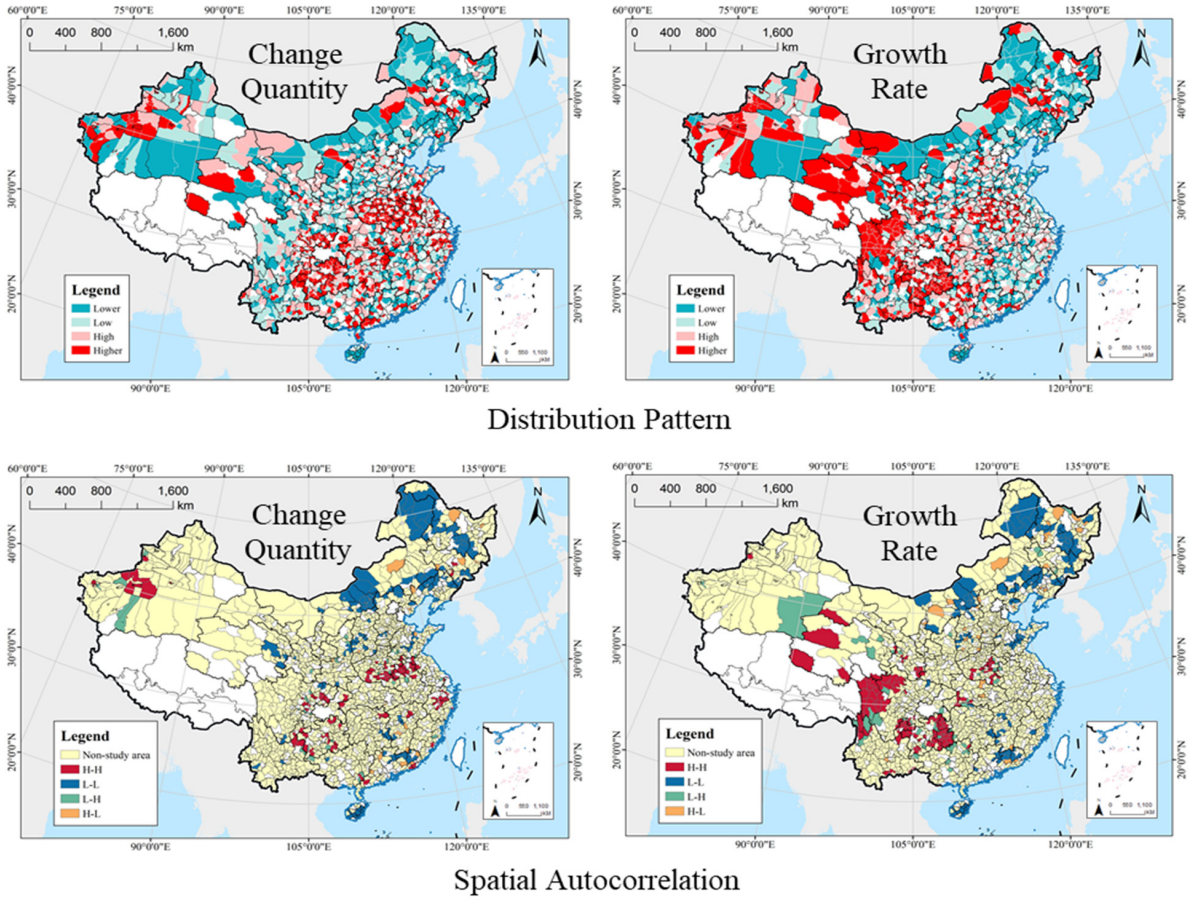


Figure 4. Distribution pattern and LISA of change quantities and growth rates for park green spaces during 2015–2024.

In addition, the park green space areas in 20 county seats remained unchanged, including Yixian, Tonghua, and Longjiang. Geographically, they are highly overlapped on both sides of the Hu Huanyong Line within the Northeast Forest Belt, Inner Mongolia Grassland Belt, Northwest Desert–Oasis Ecotone, and Southwest Karst Mountains. Administratively, the vast majority are autonomous counties or national key ecological functional areas, and they are far from provincial capitals and regional central cities.

The global Moran's index reached 0.21 ($Z = 13.11$, $p < 0.001$), indicating that the distribution of changes in park green space exhibits significant positive spatial autocorrelation, although the intensity is much lower than that of the stock. Based on a visual analysis of the local spatial autocorrelation, the HH areas were in cluster-like agglomerations, including the area where Henan, Shandong, Anhui, and Jiangsu meet (centered in the Xuzhou metropolitan area), Zhejiang (centered in the Hangzhou metropolitan area), the Chengdu–Chongqing metropolitan area, the Yunnan–Guizhou Plateau, and the western border region of Xinjiang. Most of the LL areas were concentrated in the northeast (particularly in regions adjacent to the border and the coast) and Central Inner Mongolia, in a continuous belt-like distribution. HL and LH areas are also underdeveloped, being extremely small in number and scattered in distribution (Figure 4).

3.2.2. Growth Rate of Park Green Spaces During the Research Period

For expanding county seats, the growth rate of park green spaces between 2015 and 2024 ranged from a maximum of 71.74% to a minimum of just 0.02%. Huangping and Xihua both had growth rates exceeding 70%, while Danzhai, Dancheng, Wufeng, Daozhen, and Mangya also had growth rates above 50%, giving them a clear leading advantage in the study area. Huixian had the lowest growth rate, and the growth rates of Leting, Weixian, Wuchuan, Wuchang, Huade, Benxi, Shule, and Yongfeng were also less than 1%, placing them in a severely lagging position within the study area. The average growth rate of park green spaces was 8.11%, and the median was 5.17%, indicating that a right-skewed distribution still exists (with a higher proportion of county seats experiencing slower expansion). The coefficient of variation for the growth rate of park green spaces was 1.11, and the Gini coefficient reached 0.57—far exceeding the international threshold of 0.4—indicating that the growth rate of park green spaces exhibits significant spatial heterogeneity. The results of the quantile spatial clustering analysis show that high and higher growth rates are more concentrated in the western region, especially Xinjiang, Qinghai, and Guizhou. In Central China's Henan, Hubei, and Hunan Provinces, as well as western regions such as Yunnan, Shaanxi, Sichuan, Chongqing, and Guangxi, the medium-to-high growth rate also demonstrates strong comparative advantages (Figure 4).

From 2015 to 2024, the maximum rate of decline in park and green spaces was 22.62%, and the minimum was 0.01%. Eleven county seats experienced decline rates exceeding 10%, namely Jiayin, Kulun, Jixian, Lindian, Longyao, Lianping, Zhaozhou, Wuhua, Binxian, Dongxiang, and Xingning. The decline rate in 39 county seats was less than 1%, including Chishui, Bazhou, and Kailu. The coefficient of variation for the rate of decline in park green spaces was 0.96, and the Gini coefficient reached 0.47; both are lower than the growth rate, indicating that spatial heterogeneity has decreased somewhat but remains at a relatively high level. The reduction in park green spaces was entirely classified as lower, with a more concentrated distribution in regions such as Inner Mongolia, Liaoning, Heilongjiang, Xinjiang, and Hainan (Figure 4).

The global Moran's index reached 0.28 ($Z = 17.72$, $p < 0.001$), indicating that the distribution of park green space growth rates exhibits significant positive spatial autocorrelation, although its intensity is much lower than that of the existing stock. From the perspective of the local spatial autocorrelation visualization analysis, most HH clusters are located in the border areas of Guizhou, Sichuan, and Qinghai. Most of the LL areas are concentrated in Northeastern China and Inner Mongolia, with a small portion concentrated in Guangdong and Hainan (Figure 4).

3.3. Distribution Dynamics

3.3.1. Heterogeneity Analysis

The average value of the stock index in 2024 was 11.78%, serving as the threshold for the horizontal axis. For the incremental index, zero was selected as the threshold of the vertical coordinate. Using the ISSAM, the 1760 county seats were classified into four categories. A total of 979 county seats were classified as low-stock expansion zones, accounting for more than 55% of the total. This was the type with the largest sample size. Members included Jingxing, Xingtang, and Fuping. Most were distributed in the western and northern regions, particularly in the northwest, southwest, and northeast. They were also relatively concentrated in the Beijing–Tianjin–Hebei urban agglomeration, the west coast of the Taiwan Strait urban agglomeration, and non-core cities (small and medium-sized cities that are not provincial capitals) in the Middle Yangtze River region (Figure 5).

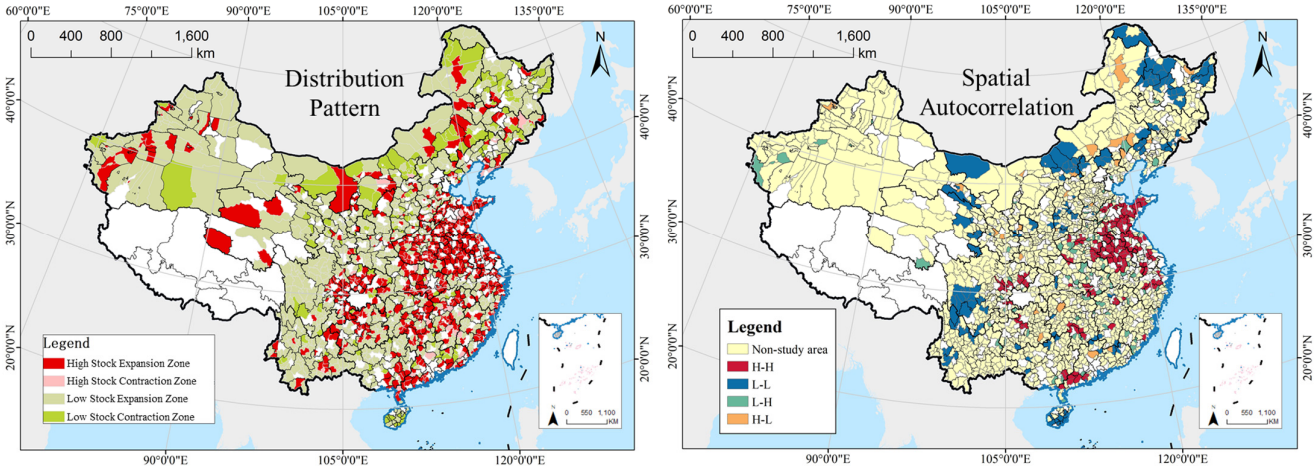


Figure 5. Distribution pattern and LISA of distribution dynamics of park green spaces during 2015–2024.

Meanwhile, 586 county seats were classified as high-stock expansion zones, accounting for 33.30% of the total. This was the type with the second-highest number of samples. Members included Gu'an, Gucheng, and Shengzhou. Most were located in the eastern and central regions, particularly in Shandong and Henan in the lower reaches of the Yellow River, with greater concentration in the Yangtze River Delta, the Chengdu–Chongqing metropolitan area, the Middle Yangtze River metropolitan area, and the Guangdong–Hong Kong–Macao Greater Bay Area. In addition, 157 county seats were classified as low-stock contraction zones, accounting for less than 10% of the total. Members included Xinfeng, Fengkai, and Dayao. Most were concentrated in the north, particularly in the northeast and Inner Mongolia, with a small number concentrated in Hainan. A total of 38 county seats were classified as high-stock contraction zones, accounting for less than 3 percent of the total. This was the type with the smallest sample size and a dispersed distribution. Members included Dalate, Changting, and Gejiu.

3.3.2. Autocorrelation Analysis

The global Moran's index was 0.35 ($Z = 20.77$, $p < 0.001$), indicating that the distribution of park green spaces exhibits significant positive spatial autocorrelation. Its intensity is higher than that of the increment but lower than that of the stock, and, to some extent, it can be regarded as a compromise between the two. Based on the visualization analysis of the local spatial autocorrelation, HH areas were largely concentrated in the lower reaches of the Yellow River Basin and extended into the Huai River Basin. Most members were distributed in Shandong and its border regions with Henan, Jiangsu, and Anhui. A small number were located in the Yangtze River Delta, Chengdu–Chongqing, and Beibu Gulf urban clusters, but they were underdeveloped. LL areas consisted of multiple small, underdeveloped clusters or stepping-stone distributions, most of which were located in the northeastern border region, Central North China and Inner Mongolia, the Loess Plateau in the northwest, the Yunnan–Guizhou Plateau in the southwest (at the border between Sichuan and Yunnan), and Hainan Island (Figure 5).

3.3.3. Robustness Test

The threshold is a key factor that affects the analysis results, and there are many methods for setting the threshold. Generally, a simpler approach is to use specific values such as the mean, median, and zero, while a more complex method is to use quantiles, natural breaks, and the K-Means algorithm for clustering analysis, which can have a significant impact. Each threshold or classification method has its advantages and disadvantages,

such as the mean being greatly affected by extreme values and the median easily ignoring detailed differences between samples. At present, China's urban construction is in a stage of transitioning from incremental development to stock development, and reduction and coordination are the focus of policy attention. Therefore, this study adopts zero and the median as thresholds, which is more in line with policy guidance. Table 3 shows that the heterogeneity and autocorrelation of the analysis results are highly robust under various threshold settings.

Table 3. Robustness testing of different thresholds.

Threshold	Mean and Zero	Median and Zero	Mean and Mean	Median and Median
High Share Expansion Zone (High Share–High Growth Zone)	586	819	205	461
High Share Contraction Zone (High Share–Low Growth Zone)	38	61	419	419
Low Share Expansion Zone (Low Share–High Growth Zone)	979	746	403	419
Low Share Contraction Zone (Low Share–Low Growth Zone)	157	134	733	461
Moran's Index	0.3477	0.3451	0.3053	0.311
Z	20.766	20.8937	18.7432	18.7275
P	0	0	0	0

3.4. Influencing Factors

3.4.1. Direction and Intensity of Factor Influence

Figure 6 shows a summary diagram of the EML analysis, indicating that the direction of influence for all factors is mixed (both positive and negative). Figure 7 presents a statistical analysis of the positive and negative SHAP values, indicating that the mixing degrees of different factors also vary significantly across different scenarios. For the high-stock expansion zone, the ratio of positive to negative SHAP values for FSSR, P, PM 2.5, and SU is roughly equal, making it a neutral factor overall. The difference between the proportions of positive and negative SHAP values among the other factors exceeds 10%. PD, GDP, T, and NSS generally have a restraining effect, while RIIS generally has a stimulating effect. Overall, PD, T, PM 2.5, and SU are neutral factors for the high-stock contraction zone; PD, GDP, FSSR, P, and NSS are inhibitory factors; and RIIS is a promotional factor. For the low-stock expansion zone, PD, RIIS, FSSR, P, PM 2.5, and SU are all neutral factors, while GDP, T, and NSS are promoting factors, with no inhibiting factors. For the low-stock contraction zone, PD, FSSR, PM 2.5, SU, and NSS are neutral factors; GDP is a promoting factor; and RIIS, T, and P are inhibiting factors.

The overall influences of different factors exhibit a significant hierarchy. For all county seats, GDP is the most critical influencing factor, with its influence far outweighing those of other factors. The ranking of PM 2.5 remains unchanged, and it is the weakest influencing factor for all county seats. The impacts of other factors vary significantly across different types of county seats. PD, FSSR, and NSS are important factors in the high-stock expansion zone, while the influences of the remaining factors are relatively weak. T, FSSR, SU, and PD are important factors for the high-stock contraction zone. PD, NSS, SU, and FSSR are important factors in the low-stock expansion zone. SU, T, PD, P, and FSSR are important factors in the low-stock contraction zone, and their influences are relatively significant.

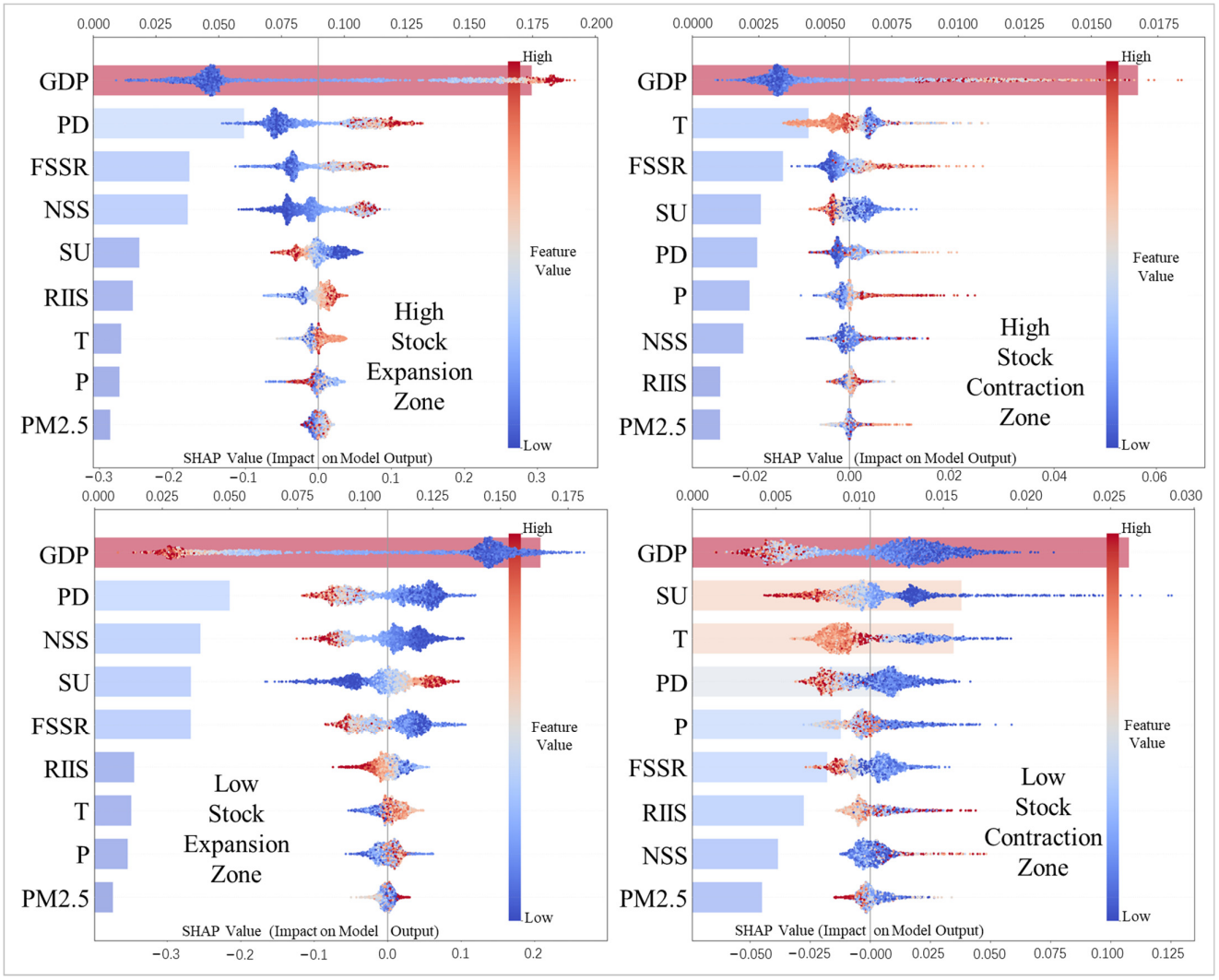


Figure 6. Summary diagram of factor influence intensity and direction.

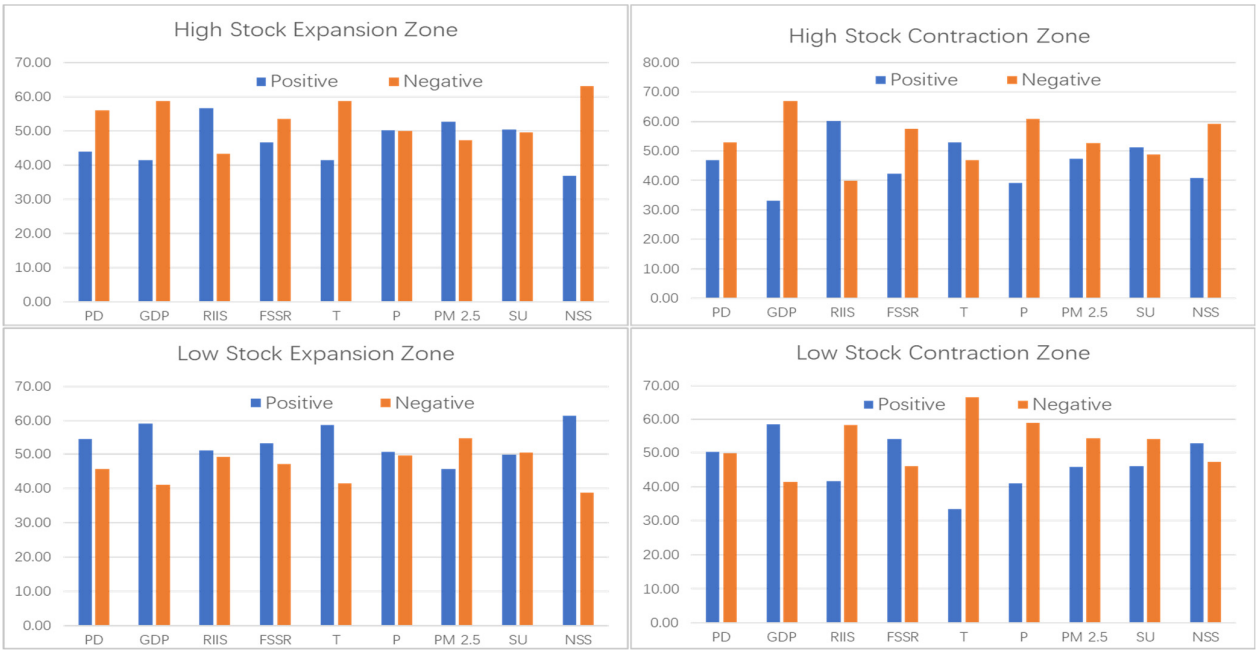


Figure 7. The ratio of positive and negative values of SHAP.

The heterogeneity in the influence of different factors in different contexts exhibits significant variation. For the high-stock expansion zone, the promoting and negative correlation effects of T, P, and SU, as well as the negative correlation effect of RIIS, all have Gini coefficients exceeding 0.4, indicating that their influences exhibit significant spatial heterogeneity. For the high-stock contraction zone, the Gini coefficients of the positive correlation effects of PD, FSSR, and P are greater than 0.4. The Gini coefficients of the promoting and negative correlation effects of RIIS, T, PM 2.5, and NSS are all greater than 0.4. For the low-stock expansion zone, the Gini coefficients of the negative correlation effects of RIIS and T, and the promoting and negative correlation effects of PM 2.5 and SU, are all greater than 0.4. For the low-stock contraction zone, the positive correlation effects of RIIS and NSS, as well as the promoting and negative correlation effects of P, PM 2.5, and SU, all have Gini coefficients greater than 0.4 (Figures 7 and 8).

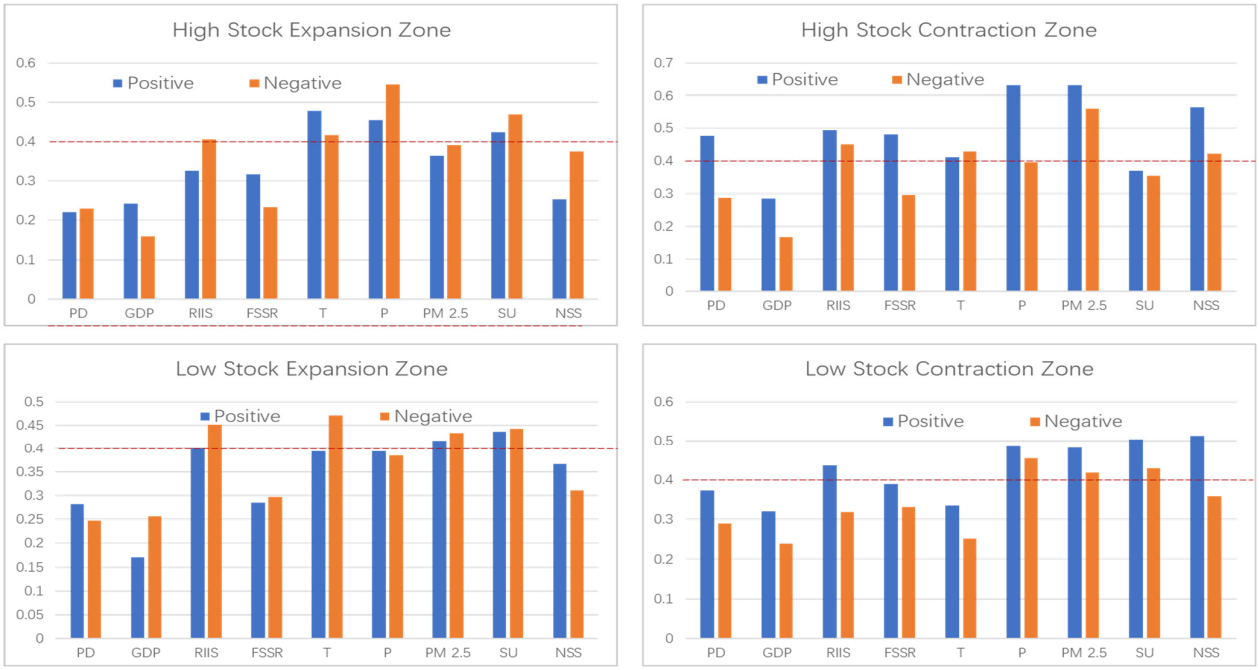


Figure 8. The Gini coefficients of SHAP (positive and negative values calculated separately).

3.4.2. Paths of Factor Influence

Figure 9 shows that the influences of all factors on the dynamic distribution of park green spaces in county seats are nonlinear, with an obvious threshold effect. The nonlinear paths of different factors exhibit significant differences. For example, regarding their impacts on the high-stock expansion zone, PD shows an inverted U-shaped pattern, while GDP shows an S-shaped pattern. The same factors also exhibit substantial variability in their impacts on different types of configuration dynamics. For example, PD exerts opposite effects on the high-stock expansion zone and the low-stock expansion zone, manifesting as an inverted U shape and a U shape, respectively. Furthermore, there are significant differences in the distribution of the thresholds at which the direction and intensity of the factor influences change. The following provides a detailed analysis of each point. To control the length, only PD, GDP, and RIIS are comprehensively analyzed, and other factors are only analyzed for key points.

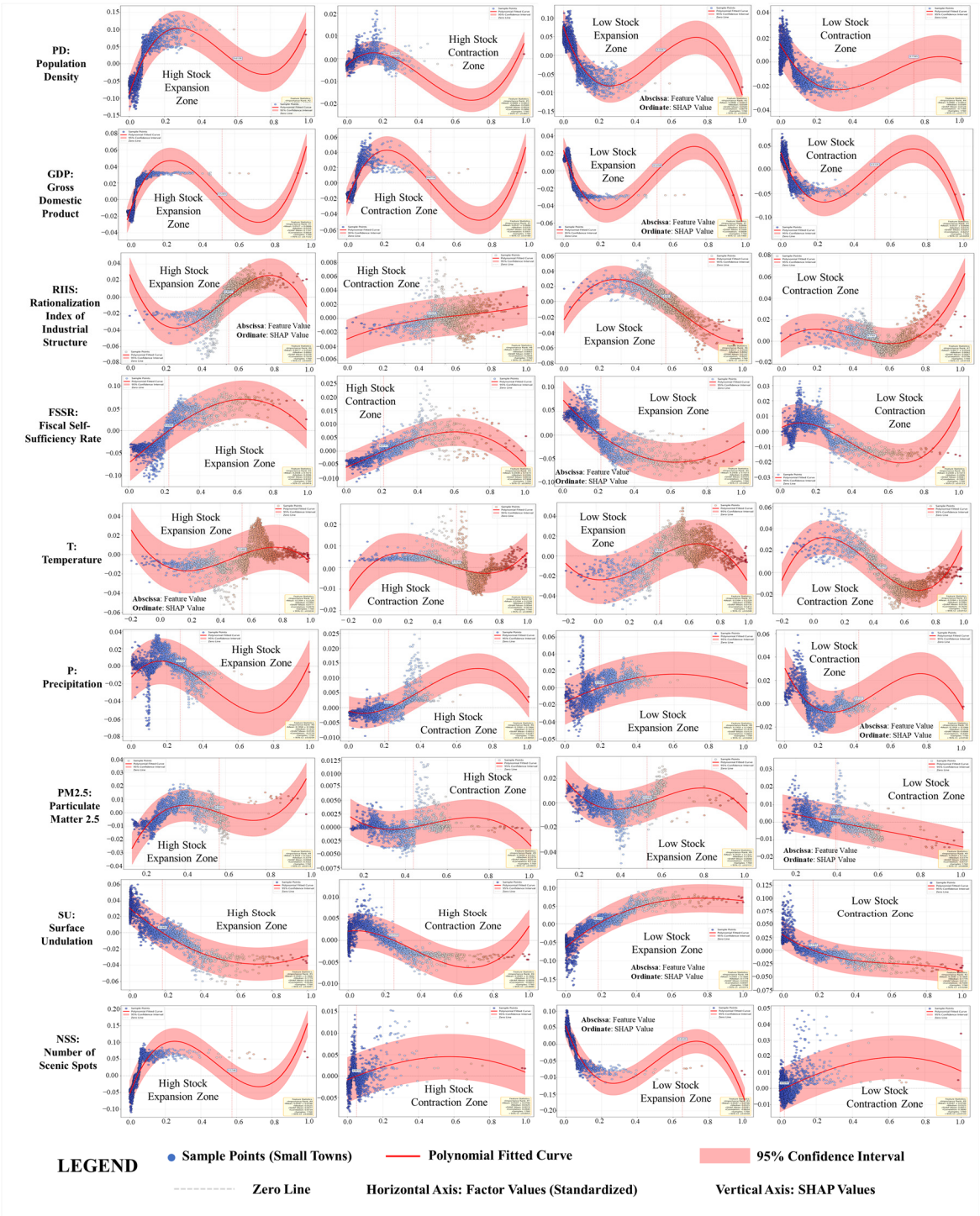


Figure 9. The impact paths of factors.

The nonlinear influence paths of PD on the high-stock expansion zone and the low-stock expansion zone are the opposite of one another, taking the shape of an inverted U and a U, respectively. At 0.06, there is a reversal in the direction of the effect. They each reach their peak influence at 0.25. The impact pathway of PD on the high-stock contraction zone also follows an inverted U shape, but its shape is smaller and relatively more developed. At 0.05, the force changes from negative to positive. At 0.27, the force transitions from positive to negative. At 0.12, the influence reaches a positive peak. The influence path of PD on the low-stock contraction zone exhibits an L-shaped pattern, with the effect transitioning from positive to negative at 0.05 and stabilizing at a high level of inhibition at 0.30. The

nonlinear influence path can be understood from the dynamic game of "demand-driven and competition crowding-out". In the low-density stage, population growth provides scale demand support for parks and green spaces, driving supply expansion, thus presenting a positive effect. However, when the density exceeds the threshold, competition for land intensifies, and the crowding-out effect of residential and industrial land on limited urban space gradually outweighs the demand effect for green space, leading to a reversal in the direction of impact. The high-stock expansion zone exhibits an inverted U shape because these areas have a relatively high degree of coordination between population agglomeration and economic development, resulting in a phased match between demand and supply. The low-stock expansion zone exhibits a U shape because, in low-stock areas with an initially insufficient population, effective demand support is lacking, and the marginal cost of public service distribution is excessively high, which inhibits green space construction. Only after crossing a threshold does the population agglomeration effect gradually emerge.

The nonlinear influence paths of GDP on the high-stock expansion zone and the high-stock contraction zone both exhibit an S-shaped pattern, but, in the final segment, the former is more convergent and the latter is more divergent. The nonlinear influence paths of GDP on the low-stock expansion zone and the low-stock contraction zone are the same, both exhibiting an L shape, but the latter is more divergent at both ends, especially at the tail end. They share the same inflection points, both transforming from negative to positive at 0.04 and stabilizing at a high value of 0.10. GDP comprehensively represents the total regional economic output and wealth creation capacity. In the low-stock expansion zone and low-stock contraction zone, an L shape is presented, indicating that the overall economic development levels of these county seats are relatively low. GDP growth has consistently been in the stage of a transition in supply capacity from "nonexistence to existence", with the wealth effect continuously being released without reaching the turning point of intensified land competition. The S-shaped pattern observed in the high-stock expansion zone and the high-stock contraction zone reflects the fact that the economic development stage in high-stock areas is more mature: early GDP growth unleashes fiscal capacity, driving the expansion of green spaces (positive trend), while, in the mid-stage, economic prosperity triggers intensive urban development, and the crowding-out effect of commercial and residential land on green spaces becomes dominant (reversal of direction); in the late stage, as economic development enters an advanced phase, residents' demand for ecological quality rebounds, once again driving the expansion of green spaces, thereby forming a complete S-shaped evolutionary trajectory.

RIIS exhibits an N-shaped nonlinear influence path on the high-stock expansion zone, transitioning from negative to positive at 0.81. At both ends, the data are highly dispersed, especially at the starting end, with many data points falling outside the confidence interval. The effect of RIIS on the high-stock contraction zone is nearly linear, with a reversal in the action direction at 0.77. The path pattern exhibits a strong tendency toward divergence overall, particularly at the end, where a large number of data points have moved outside the confidence interval. The nonlinear effect of RIIS on the low-stock expansion zone follows an inverted U-shaped curve, with the peak influence occurring at 0.68. At 0.81, the direction of influence reverses from positive to negative. The nonlinear impact path of RIIS on the low-stock contraction zone exhibits a roughly U-shaped pattern, with the trough located at 0.84. The direction of the effect changes from positive to negative at 0.78 and from negative to positive at 0.87. RIIS takes an inverted U-shape in the low-stock expansion zone and a U-shape in the low-stock contraction zone, indicating that the land available for redevelopment—released during the early stages of industrial restructuring in low-stock areas—can provide phased support for green space expansion. However, the revaluation of land value resulting from industrial upgrading will rapidly strengthen the competitive ad-

vantage of non-green functional land, prompting the reversal of this trend. The high-stock expansion zone exhibits an N-shaped pattern, stemming from the multistage fluctuations that occur in these areas during industrial restructuring—specifically, the alternating cycles of "industrial upgrading creating demand for ecological space, intensified competition for land displacing green spaces, and the clustering of high-end service industries enhancing ecological quality". The high-stock contraction zone is approximately linear. Due to the solidification of the industrial structure in these regions, the adjustment space is limited. The changes in RIIS reflect stock optimization rather than structural transformation, with a weak influence and stable direction.

FSSR exhibits an inverted U shape in the high-stock expansion zone and a U shape in the low-stock expansion zone, reflecting the different constraints faced by regions with varying financial resource bases. A higher FSSR frees up more funds for green space development in the early stages; however, when local governments become overly reliant on land sale revenues, a high self-sufficiency rate actually strengthens the incentive to rely on land-based revenues, prompting governments to allocate scarce land to development projects that generate direct fiscal returns, thereby curtailing green space development. For regions with insufficient financial resources, they must first cross the fiscal threshold required for basic operations before the remaining financial resources can be gradually allocated to non-urgent ecological welfare. The high-stock contraction zone and the low-stock contraction zone exhibit a parabolic shape with opposite directions, revealing that minor improvements in fiscal autonomy within fiscal contraction zones have distinctly different marginal effects on green space maintenance or decline, depending on the region's fiscal vulnerability interval.

T exhibits a wavy pattern across all four zones, reflecting the dual constraints that temperature places on green spaces. When the rise in temperature exacerbates the heat island effect, residents' demand for green space cooling services surges, triggering policy responses that promote green space expansion, resulting in multistage alternating wave-like fluctuations. The systematic shifts in thresholds across different regions reflect the differences in the local climatic background and urban thermal environment baselines.

The differences in P pathways across different subregions stem from variations in baseline moisture conditions and the marginal ecological effects of precipitation changes in different areas. In semi-arid regions with insufficient moisture, the marginal positive correlation effect of increased precipitation on green space construction is extremely significant. However, beyond a certain threshold, or in humid regions, excessive precipitation transforms ecological benefits into maintenance burdens.

PM2.5 serves as an external environmental constraint faced by green space configuration and also constitutes an implicit signal of residents' demand for green space ecological services. Its role is characterized by a two-way interaction. PM2.5 exhibits an N-shaped pattern in the high-stock expansion zone, a wavy pattern in the high-stock contraction zone and low-stock expansion zone, and a linear pattern in the low-stock contraction zone, reflecting the differentiated transmission logic of air pollution on green space distribution at different stages of development. In the initial stage, the rise in PM2.5 reflects accelerated industrialization and urbanization, as well as the reduction of green spaces, thus showing a negative trend. When pollution surpasses the residents' tolerance threshold, public environmental demands compel the government to increase the supply of green infrastructure, thereby transforming pollution pressure into a driver for green space expansion, with the effect shifting from negative to positive. As pollution continues to worsen to severe levels, local governments face a trade-off in allocating financial resources between combating smog and creating green spaces; the urgent need to combat smog may crowd out investment in green spaces, causing the effects to reverse once again. The low-stock

contraction zone exhibits a linear negative trend, indicating that these marginalized areas are constrained by both fiscal capacity and governance levels, and the logic of pollution crowding out green space has never been interrupted by effective policy responses.

The nonlinear influence paths of SU on the high-stock expansion zone and low-stock expansion zone are both arc-shaped but in opposite directions, revealing the alternating dominance of the "construction cost effect" and the "landscape premium effect" of terrain on green space distribution. When the initial terrain is flat, development costs are low; however, land use competition is intense and green space distribution is given low priority. As the degree of undulation increases, mountainous and hilly areas that are unsuitable for high-intensity development are instead left as blank spaces due to construction constraints, providing "passive protection" for green spaces, and the effect shifts from negative to positive. The nonlinear influence path of SU on the high-stock contraction zone exhibits a parabolic shape. This reflects the fact that the construction and maintenance costs brought about by the topographic relief in the stock contraction area are further amplified against the background of the continuous decline in existing green space, forming a positive feedback lock-in consisting of "the more complex the terrain, the more severe the degradation".

NSS serves as an indicator of regional ecological baseline quality and the concentration of natural tourism resources; it influences the logic of green space distribution through paths such as tourism-driven economic growth, the ecological brand effect, and the enhancement of residents' aesthetic awareness. NSS exhibits L-shaped nonlinear influence paths for both the high-stock expansion zone and the low-stock expansion zone, but their directions are the opposite. Their thresholds are essentially the same, shifting from negative to positive or positive to negative at 0.05, and the influence stabilizes after exceeding 0.07. This suggests that a small number of scenic areas is not enough to alter the basic logic governing the distribution of green spaces in a region; however, once a threshold is crossed, the enhanced ecological awareness and policy demonstration effects brought about by these scenic areas begin to take effect, driving the expansion of green spaces. If scenic areas are too densely concentrated, the substitution and diversion effects of tourism spending from outsiders on local public green spaces become significant. Local governments tend to focus their investments on core scenic areas rather than on scattered urban parks and green spaces, resulting in the persistent crowding-out effect of the number of scenic areas on the distribution of urban green spaces. The nonlinear influence paths of NSS on the high-stock contraction zone and the low-stock contraction zone are similar, both appearing as arcs.

4. Discussion

4.1. Comparison with Existing Studies

In existing studies, scholars have systematically examined the spatial characteristics of urban green space distribution using multiple econometric models, and they have revealed its influencing mechanisms from multiple dimensions, such as economy, society, governance, policy orientation, and natural ecology [58]. Based on an empirical analysis of a nationwide large-scale county seat-level sample, this study validates some conclusions drawn from small samples or specific regions and also reveals several new findings that differ from, or even contradict, existing understandings.

4.1.1. Common Features

With regard to common findings regarding the characteristics of green space distribution, this study confirms that, between 2015 and 2024, the dynamics of park and green space distribution across 1760 county seats in China exhibited significant imbalances, inequities, and spatial autocorrelation in terms of existing stock, new additions, and their interrelationships. This conclusion is highly consistent with the existing literature. A large number of

scholars have used the Gini coefficient and Moran index to analyze the spatial heterogeneity and correlations of green space distribution. For example, Wang's case analysis of London suggests that a Gini coefficient of less than 0.25 indicates high fairness in non-park green space distribution, while a Gini coefficient greater than 0.4 indicates severe deprivation [59]. Yuan [15] pointed out, in a study on 11 representatives county seats in Sichuan Province, that there is significant positive spatial autocorrelation in green land use efficiency, and its intensity shows a decreasing trend. This study further discovered that, although the global Moran's I of park green space at the national level has gradually decreased, it remains at a relatively high level. This finding not only validates the above viewpoint but also effectively extends it to the national scale.

Similarly, Wang [39] evaluated the significant inequality in the spatial patterns of green spaces across 314 Chinese cities based on the Gini coefficient and Moran's I. He also pointed out that factors such as the population size and housing prices have nonlinear threshold effects and saturation effects. Cai [40] found that urban green spaces along the Grand Canal exhibit significant spatial heterogeneity and autocorrelation and are synergistically influenced by multiple factors, including the population, aging, and the economy. Huang [17] argues that most large cities in China face issues of insufficient green space supply and unfair distribution, and their spatial autocorrelation is comprehensively influenced by the natural conditions, economic growth, urbanization, land finance, and the land transfer system. Cross-national studies also support this universality. Ajmi and Li [60] revealed the uneven spatial distribution of the quantity and quality of green spaces. Faka [14] mapped green space inequality in the capitals of 26 European countries and found significant heterogeneity both between and within cities, with Northern Europe showing greater equity than Southern Europe. Roodsari [61] also found an uneven distribution of green spaces in a case study of Tehran, Iran, suggesting that this may be a challenge faced by the entire world. The above evidence from both China and other countries collectively indicates that the inequality and spatial autocorrelation of park green space distribution exhibit cross-regional universal characteristics across different scales and institutional contexts. These characteristics are common patterns applicable to both large and small cities, as well as to China and non-China settings.

4.1.2. Influencing Consensus

At the level of influencing factors, there are also many intersections between the existing achievements and this study. In terms of factor composition, Zhang [62] found that temperature, topographic relief, altitude, PD, and construction intensity are the main factors affecting green space change in the Chengdu–Chongqing Economic Circle. He also argued that the influences of natural factors diminish over time, while those of human social factors significantly intensify. Yang [63] and Wang [64] believe that economic development, PD, transportation patterns, and local environmental quality are key external factors affecting green space change and equity in large cities. Li [65] conducted an empirical analysis of 58 representative cities in China and concluded that spatial equity in urban green spaces in China is poor, with climate, topography, and PD being key influencing factors.

As for the intensity of these influences, Huang [66] analyzed the dynamics of urban green spaces in Africa from 2000 to 2024 and their influencing factors using remote sensing technology. The study found that socioeconomic factors played a particularly prominent role and concluded that the intensity of these factors' influences and their influencing factors vary by region. Kasahun [67] suggested that factors such as PD, slope, altitude, and proximity to rivers are important determinants of urban green space distribution in Ethiopia. Wei [68] argued that the influence of socioeconomic factors on the spatial

patterns and changes in global urban green spaces is far greater than that of natural environmental factors.

Regarding the direction of influence, Liu [69] argued that socioeconomic factors present both positive promoting effects and negative pressures, with significant spatial and temporal variability. Chang [70] pointed out that the rationalization and optimization of the industrial structure have a positive effect for regenerative cities, growing cities, and declining cities but a negative effect for mature cities.

Regarding the pathways of effects, Ji [36] conducted an empirical analysis of changes in green space over different time periods using a geographically weighted regression model. The study showed that the nature of the impact of socioeconomic factors on green space undergoes a reversal; for example, the effect of PD shifts from inhibitory to promotional. Li [71] suggested that precipitation, built-up areas, and other factors are key determinants of the spatial patterns of urban green space coverage and tested the nonlinear relationships and marginal effects of the factor paths using a random forest model.

4.1.3. Divergence and Contributions

Notably, this study also reveals some findings that diverge significantly from the existing literature, and these controversial points merit further exploration in the future. For example, regarding the changing trend of Moran's I, this study finds that the global Moran's I of park green space configuration in county seats tend to decline overall, while Shi [72], in a study on Suzhou, found an upward trend (from 0.33 to 0.49). Similarly, Lian [11] suggested that PD has a positive promoting effect on the evolution of green space patterns. Wang [73] stated that PD is a key factor influencing changes in urban green spaces in Jinan, Shandong. Li [74] holds that PD is a key factor influencing the evolution of green space utilization efficiency in resource-based cities and argues that the influence of economic indicators is gradually weakening. Doan [75] found that economic and demographic factors have a significant impact on the spatiotemporal evolution of green spaces in Vietnam, concluding that PD is the decisive factor, while the economy plays a positive promoting role. Nor [76] suggests that PD and the spatial structure are key factors influencing the evolution of urban green spaces in Southeast Asia, and their impacts are greater in Jakarta and Greater Manila. In contrast, the empirical results of this study, based on a nonlinear EML model, demonstrate that social demand, economic supply, and natural ecological factors all carry both positive and negative bidirectional effects. The introduction of the threshold effect and inflection point identification has significantly improved the model's fitting accuracy and interpretability and further facilitates the precise translation of analytical conclusions into policy practice, providing a more reliable basis for decision-making regarding differentiated regulatory strategies.

4.2. Inspiration and Suggestions

4.2.1. Zoning Management: Shifting from Industry-Based Management to Spatial Governance

Based on the empirical results of the ISSAM, the 1760 county seats were classified into four significantly different spatial types. In future management, it is necessary to break through the traditional boundary of landscaping and turn to the design of spatial governance policies with the distribution of spatial resources as the core, designing differentiated management policies by region based on the results of matrix classification [77,78]. With regard to the high-stock expansion zone, the policy focus should shift from "quantitative accumulation" to "qualitative benchmarks". It is recommended to leverage the advantages of high stock to apply for national-level "Garden City" and "Forest City" certifications, create a regional-level "Park City" model, and strengthen its radiating and driving effects on the surrounding areas [79]. For the low-stock expansion zone, it is necessary to

be vigilant against excessive supply that is divorced from the actual demand, and policies should focus on supply-matching regulation. The recommendation is to establish a dynamic monitoring and early warning mechanism for "population–economy–green spaces" to strictly control the excessive distribution of green spaces that is not aligned with population needs and the economic carrying capacity. This will ensure that additional investments are targeted precisely at addressing shortcomings and prevent the waste of park and green space resources [80]. For the high-stock contraction zone, the core of the policy lies in bottom-line management and urban physical examination. It is suggested that the diagnosis of park green space erosion be carried out as soon as possible, with a focus on identifying key nodes where urban built-up area park green spaces have been encroached upon or degraded. Ecological restoration should be implemented through measures such as vertical greening and the revitalization of marginal land [81,82]. Moreover, it is necessary to draw on the experience of ecological control line planning and management in Shenzhen to establish a system and mechanism to curb the continuous decline of park green spaces. The low-stock contraction zone should be designated as a priority area for policy and external intervention, and a rescue strategy that emphasizes both the revitalization of existing stock and the injection of new stock should be implemented [83]. Policy design should break down departmental silos; coordinate resources from housing and urban–rural development, natural resources, and finance departments; and address marginalized lock-in through exploiting existing potential (e.g., building pocket parks on leftover land) and external infusion (external transfer payments and policy preferences).

4.2.2. Staged Management: Shifting from Static Oversight to Dynamic Early Warning

The nonlinear, complex interaction processes and threshold values of the various factors identified through SHAP interpretable machine learning suggest that green space governance should abandon the static unified control model and instead adopt phased, time-sequential dynamic early warning management strategies [84]. All regions should establish an early warning threshold system based on the inflection point values of key factors such as the local population, economy, and climate and take measures to correct inequalities in planning, design, and management policies [9]. It is important to accurately distinguish between the different stages—such as the low-activity phase, the saturation phase, and the phase of directional change—and to implement tailored intervention strategies accordingly. When indicators such as the regional GDP and PD approach the threshold for green space supply, plans for new park land should be created in advance. If the industrial structure and development intensity exceed the critical values at which green space is suppressed, it is necessary to immediately delineate ecological buffer and green space protection control lines [85]. For natural constraint factors such as PM2.5 and terrain, green construction standards should be adjusted based on their impact inflection points. A routine, dynamic monitoring and early warning mechanism should be established to predict trends in the stock and growth of green spaces based on the nonlinear evolution patterns of relevant factors. This will shift the management model from the passive governance of post-event remediation to the proactive spatial control of pre-event prediction and precise intervention, achieving the long-term, balanced distribution of park green space resources in county seats.

4.2.3. Graded Management: Shifting from a One-Size-Fits-All Approach to a Tailored Approach

Based on the EML (SHAP) analysis results, the nine influencing factors exhibit significant hierarchical differentiation in their importance for park green space configuration, and the strength of effect of the same factor demonstrates marked spatial heterogeneity across different regions. Traditional uniform benchmark management can no longer adapt to the

complex realities, necessitating the graded management of factors and regions to promote precise, locally tailored policy shifts [86]. Based on the SHAP importance measure, the nine influencing factors are categorized into three levels: critical, important, and auxiliary. Key factors should be included in the core regulatory list, with routine monitoring and proactive early warning implemented. Important factors should serve as leverage for phased policy adjustments, intervening at opportune times in conjunction with threshold effects. Auxiliary factors, on the other hand, focus primarily on adaptive management, emphasizing dynamic monitoring rather than rigid control [40]. Moreover, the planning, layout, construction, and management of park green spaces should be regarded as the primary objective of spatial planning. The non-stationarity of factor effects should be fully understood and utilized to promote a more scientific approach to green space supply and management [87]. In "hot spots" where the influence of these factors is strong, the focus is on consolidating strengths and setting benchmarks. In "blind spots" or "negative zones" where the influence of certain factors is weak, it is necessary to conduct an in-depth analysis of the paths causing these blockages and implement targeted policies to address them and allocate resources accordingly.

4.3. Contributions and Limitations

4.3.1. Scientific Contributions and Practical Implications

First, the methodological contribution lies in introducing EML models, thereby constructing a nonlinear, interpretable evidence chain for the dynamic formation paths of small-town park green space distribution. This study integrates EML (SHAP) with the Geographical Detector, GWR, and ESDA, enabling the model to first learn complex structures and then quantify the marginal contributions of each factor according to game theory-based distribution logic. This approach simultaneously incorporates nonlinear relationships, threshold effects, and spatial heterogeneity into the chain of evidence, mitigating the bias in path identification inherent in single-tool approaches. It refines the quantitative analysis paradigm for the influencing factors of park green spaces and provides a reusable technical framework for nonlinear research related to ecological spatial configuration.

Second, the analytical framework contributes to the development of a synergistic analysis matrix for existing and incremental resources, advancing the dynamic study of park green space distribution in county seats from "describing changes" to "diagnosing types". Moreover, the study proposes an analytical tool that better aligns with the policy orientation of "coordinating the comprehensive land supply of both stock and increment". Furthermore, by combining ESDA and EML applications, a new research route for the configuration of park green spaces in county seats has been constructed from a global perspective, integrating "type diagnosis–spatial effect–nonlinear path" into an integrated analysis framework.

Finally, the spatial scale focuses on county seats, thereby narrowing the scope of analysis and refining the level of detail. By focusing on this systematically marginalized spatial unit, this study reveals its unique configuration patterns and influencing factors, providing decision-making support that is of greater practical value for the planning and management of park green spaces in the vast number of similar county seats and further expanding the scale and framework of research on urban green spaces.

4.3.2. Research Limitations and Future Research Needs

Constrained by factors such as data availability and the capacity of the research team, this study inevitably has certain limitations. For example, per-capita urban green space is one of the oldest and most widely used indicators in urban planning, but this study was unable to include the indicator of the per-capita park green space area, making it difficult to

accurately reflect the actual level of access for residents. There is also a lack of examination of the internal spatial distribution pattern and plot morphology of park green spaces within the county seat area, which may have resulted in neglecting inequality issues within county seats. The limitations above may affect the precision of policy targeting. Future studies will focus on collecting data on the distribution of green spaces within county seats and detailed population distribution data. This will involve, for example, integrating POI and mobile phone signaling data with multitemporal remote sensing imagery and applying multiscale analytical methods to further elucidate the micro-level equity in the distribution of park green spaces in county seats and the paths underlying their formation.

5. Conclusions

This study examined 1760 county seats in China. By combining the ISSAM, ESDA, and EML (SHAP) methods, it systematically revealed the spatiotemporal patterns, spatial correlation characteristics, and nonlinear paths of influencing factors in the spatial distribution of park green spaces in county seats from 2015 to 2024, thereby providing empirical evidence for the governance of urban green spaces.

Key findings are as follows:

(1) There is significant, dynamic type differentiation in the configuration. Based on the ISSAM, 1760 county seats were categorized into four types, providing clear targets for targeted regional governance. Low-stock expansion zones (979, 55.6%) are dominant by low stock but expanding increment, mostly distributed in the western, northern, and non-core urban agglomerations. High-stock expansion zones (586, 33.3%) are the dominant type, featuring the coordinated growth of stock and increment, concentrated in the eastern coastal areas and core city clusters. Low-stock contraction zones (157, 8.9%) are marginalized, with both low stock and low increment, mainly concentrated in Northeastern China and Inner Mongolia. High-stock contraction zones (38, 2.2%) are a type at risk of degradation, characterized by high stock but shrinking increment, scattered across various locations. Although small in number, they should not be overlooked.

(2) Spatial heterogeneity and autocorrelation coexist. The stock distribution exhibits a gradient pattern of "high in the east and low in the west". Incremental expansion has accelerated in the central and western regions, but spatial imbalance has become more pronounced (Gini coefficient: 0.53). The global Moran's I index shows that the stock (0.40 and 0.45), increment (0.21), and distribution dynamics (0.35) all exhibit significant positive spatial autocorrelation, but the clustering intensity of the increment and distribution dynamics is notably weaker than that of the stock, indicating that incremental intervention has considerable spatial regulation potential. The overall pattern of regional agglomeration remains stable, but the LL zone is contracting in the west and expanding in the northeast, while the HH zone is extending toward the lower reaches of the Yellow River and the Chengdu–Chongqing metropolitan area.

(3) The influence paths of factors exhibit complex, nonlinear characteristics. The SHAP model identifies four characteristics of factor effects. First, there is a mixed direction of effects; for example, both the population density (PD) and GDP contribute both positively and negatively to changes in green space. Second, the impact is categorized by intensity; for example, GDP is the key factor among all types, while PM2.5 is consistently the weakest auxiliary factor. Third, the action path is nonlinear, covering diverse curve shapes, such as inverted U-shaped, U-shaped, S-shaped, N-shaped, L-shaped, and wavy shapes. Threshold effects are ubiquitous, and the inflection point values vary significantly by factor and region type. For instance, PD exhibits an inverted U-shaped effect on high-stock expansion areas, while it demonstrates a U-shaped

effect on low-stock expansion areas. Fourth, regional heterogeneity should be noted: the influence intensity and threshold of the same factor vary greatly across different configuration type areas, and the Gini coefficients of about half of the factors exceed 0.4, reflecting their spatial non-stationarity. For example, RIIS follows a U-shaped path in low-stock shrinking areas but an N-shaped path in high-stock expanding areas.

(4) Based on the results of the empirical analysis, this study proposes management strategies following a "zoning–grading–staging–synergy" approach. Based on the results of the ISSAM, zoning requires the design of differentiated policies—such as prioritizing quality in areas with high housing stock and focusing on emergency measures in areas with low housing stock and declining populations—to gradually facilitate the transition from landscape industry management to spatial governance. Grading requires implementing tiered management and location-specific adjustments based on the severity of factor impacts and spatial heterogeneity. Staging requires the establishment of a dynamic early warning mechanism based on the complex, nonlinear pathways and threshold values of factor interactions, enabling proactive intervention before a turning point is reached. Synergy requires integrating spatial autocorrelation characteristics, breaking down administrative barriers, and establishing a new framework for cross-regional alliance-based green space governance.

Author Contributions: Conceptualization, B.Z. and J.X.; methodology, S.Z. and B.Z.; software, S.Z.; validation, B.Z., J.X., and S.Z.; formal analysis, J.X.; investigation, B.Z. and J.X.; resources, B.Z. and J.X.; data curation, B.Z. and S.Z.; writing—original draft preparation, B.Z. and J.X.; writing—review and editing, S.Z. and B.Z.; visualization, S.Z.; supervision, J.X.; project administration, B.Z. and J.X.; funding acquisition, B.Z. and J.X. All authors have read and agreed to the published version of the manuscript.

Funding: This research was funded by the General Program of the National Natural Science Foundation of China, grant number 52478046.

Data Availability Statement: The data were obtained from the China County Seat Construction Statistical Yearbook and the China Urban Construction Statistical Yearbook, which are published by the Ministry of Housing and Urban–Rural Development of the People's Republic of China. Additional data were sourced from the China Statistical Yearbook (County-Level) and the China City Statistical Yearbook, which are published by the National Bureau of Statistics of China.

Acknowledgments: The authors are grateful for Zhou's help in improving the quality of the figures.

Conflicts of Interest: The authors declare no conflicts of interest.

Abbreviations

The following abbreviations are used in this manuscript:

PGS	Park Green Space
ISSAM	Stock and Incremental Synergy Analysis Matrix
ESDA	Exploratory Spatial Data Analysis
EML	Explainable Machine Learning
PD	Population Density
GDP	Gross Domestic Product
RIIS	Rationalization Index of Industrial Structure
FSSR	Fiscal Self-Sufficiency Rate
T	Temperature
P	Precipitation
PM2.5	Particulate Matter 2.5
SU	Surface Undulation
NSS	Number of Scenic Spots

References

1. Panwar, M.; Mina, U.; Kumar, K.; Kumar, M. Urban green space assessment index (ugsai): A novel gis-based measure for assessing green spaces in Delhi. *Environ. Urban. Asia* **2025**, *16*, 122–142. [CrossRef]
2. Tate, A. Urban parks in the twentieth century. *Environ. Hist.* **2018**, *24*, 81–101. [CrossRef]
3. Hassan, Y.N.; Jombach, S. Urban green space per capita for sustainable and equitable urban planning: A systematic review and bibliometric analysis. *Land* **2025**, *15*, 29. [CrossRef]
4. Godoi, N.M.I.; Gomes, R.C.; Longo, R.M. Contributions of urban green spaces to cities: A literature review. *Sustain. Environ.* **2025**, *11*, 2464418. [CrossRef]
5. Halecki, W.; Stachura, T.; Fudala, W.; Stec, A.; Kubon, S. Assessment and planning of green spaces in urban parks: A review. *Sustain. Cities Soc.* **2023**, *88*, 104280. [CrossRef]
6. Alfarhood, M.; Alahmad, A.; Alalwan, A.; Alkulaib, F. Leveraging satellite imagery and machine learning for urban green space assessment: A case study from Riyadh city. *Sustainability* **2025**, *17*, 6118. [CrossRef]
7. Cissé, M.; Morenikeji, O.; Mertens, E.; Fall, A.N.; Okhimamhe, A.A. Assessment of green space dynamics under urban expansion of senegalese cities: The case of Dakar. *Urban Sci.* **2024**, *8*, 258. [CrossRef]
8. Korah, P.I.; Akaateba, M.A.; Akanbang, B.A.A. Spatio-temporal patterns and accessibility of green spaces in Kumasi, Ghana. *Habitat Int.* **2024**, *144*, 103010. [CrossRef]
9. Gül, A.; Dinç, G.; Aydemir, Ç. Analysis of urban green space inequalities in Isparta, Turkey. *TeMA-J. Land Use Mobil. Environ.* **2024**, *2*, 47–63. [CrossRef] [PubMed]
10. Ayele, B.Y.; Megento, T.L.; Habetemariam, K.Y. The governance and management of green spaces in Addis Ababa, Ethiopia. *Heliyon* **2022**, *8*, e09413. [CrossRef] [PubMed]
11. Huang, B.H.; Gu, J.T.; Zhang, M.F.; Feng, Z. Green space equality is better in fast-growing cities: Evidence from 140 cities in China. *Land* **2025**, *14*, 366. [CrossRef]
12. Qin, Y.T.; Ma, Y.B.; Gong, M.J.; Li, S.D.; Chen, P.F. Investigating the serviceability of urban green spaces from a spatial perspective: A comparative study across 368 cities on the Chinese mainland. *Land* **2025**, *14*, 711. [CrossRef]
13. Kukulska-Koziel, A.; Starczewski, T.; Rogatka, K.; Cegielska, K.; Noszczyk, T.; Mlocek, W. Urban green space provision dynamics. A cross-European analysis of supply, availability, and land cover flows in capitals. *Urban For. Urban Green.* **2026**, *121*, 129474. [CrossRef]
14. Faka, A. Mapping green space inequalities in 26 European cities. *Land* **2025**, *14*, 2362. [CrossRef]
15. Yuan, T.; Zhang, J.; Xiang, Y.; Lu, L.Y. Exploring the temporal and spatial evolution laws of county green land-use efficiency: Evidence from 11 counties in Sichuan province. *Buildings* **2022**, *12*, 816. [CrossRef]
16. Pan, X.T.; Wu, S.N.; Zhang, X.L. How green space quality influences fiscal stress: A multidimensional perspective. *J. Urban Plan. Dev.* **2025**, *151*, 04025039. [CrossRef]
17. Shackleton, C.M.; Blair, A.; De Lacy, P.; Kaoma, H.; Mugwagwa, N.; Dalu, M.T.; Walton, W. How important is green infrastructure in small and medium-sized towns? Lessons from South Africa. *Landsc. Urban Plan.* **2018**, *180*, 273–281. [CrossRef]
18. Hofman, M.; Simácek, P. Placemaking for urban green spaces: Journey towards a better public space. *Morav. Geogr. Rep.* **2026**, *34*, 2–13. [CrossRef]
19. Ajmi, R.; Boussema, S.B.F.; Taîbi, A.N.; Allouche, F.K.; Khessibi, A.; Essassi, S.; Mechmech, Y.; El Jenzri, K.; Gaafar, O.; Mezeres, J.L. Assessing the distribution of public urban green space: A combined geographical-quality approach in a Mediterranean city. *Euro-Mediterr. J. Environ. Integr.* **2026**, *11*, 79. [CrossRef]
20. Roslan, N.; Marzbali, M.H.; Abdullah, A.; May, A.S. Mapping access to green space in Penang, Malaysia: A GIS-Based Study. *Rev. Int. Geomat.* **2025**, *34*, 553–567. [CrossRef]
21. Agustiyara, A.; Mutiarin, D.; Nurmandi, A.; Kasiwi, A.N.; Ikhwali, M.F. Mapping urban green spaces in Indonesian cities using remote sensing analysis. *Urban Sci.* **2025**, *9*, 23. [CrossRef]
22. Kifayatullah, S.; Saqib, Z.; Khan, M.I.; Zaman-ul-Haq, M.; Kucher, D.E.; Ullah, S.; Tariq, A. Equitable urban green space planning for sustainable cities: A GIS-based analysis of spatial disparities and functional strategies. *Sci. Rep.* **2025**, *15*, 22686. [CrossRef]
23. Zhao, W.; Liu, D.F.; Niu, J.Q.; He, J.H.; Xu, F. Spatial heterogeneity analysis of the multidimensional characteristics of urban green spaces in China-A Study Based on 285 Prefecture-Level Cities. *Land* **2024**, *13*, 1050. [CrossRef]
24. Wu, Y.L.; Luo, M. Study on spatial-temporal evolution law of green land use efficiency in resource-based cities. *Land* **2025**, *14*, 360. [CrossRef]
25. Peng, W.Y.; Sun, Y.; Li, Y.C.; Yuchi, X.J. An evaluation and promotion strategy of green land use benefits in china: A case study of the Beijing-Tianjin-Hebei Region. *Land* **2022**, *11*, 1158. [CrossRef]
26. Misty, M.S.; Hoque, M.A.; Mukul, S.A. Assessment of urban green space dynamics in Dhaka South city corporation of Bangladesh using geospatial techniques. *Land* **2024**, *13*, 1426. [CrossRef]
27. Bizuayehu, G.; Gashu, K.; Debebe, B. Spatiotemporal dynamics of urban green spaces and land use/land cover change in Gondar City, Amhara Region, Northwest Ethiopia. *J. Landsc. Ecol.* **2026**, *19*, 53–78. [CrossRef]

28. Fikri, H.Z.; Hasibuan, H.S.; Setiowati, R. Spatiotemporal dynamics and economic valuation of urban green space in transit-oriented development. *Glob. J. Environ. Sci. Manag.-GJESM* **2025**, *11*, 1591–1612. [CrossRef]
29. De Lima, G.N.; Fonseca-Salazar, M.A.; Campo, J. Urban growth and loss of green spaces in the metropolitan areas of Sao Paulo and Mexico City: Effects of land-cover changes on climate and water flow regulation. *Urban Ecosyst.* **2023**, *26*, 1739–1752. [CrossRef]
30. Jia, Y.F.; Chen, Z.F.; Lu, X.H.; Sheng, S.; Huang, J.D.; Wang, Y.C. The degradation and marginal effects of green space under the stress of urban sprawl in the metropolitan area. *Urban For. Urban Green.* **2024**, *95*, 128318. [CrossRef]
31. Sathyakumar, V.; Ramsankaran, R.; Bardhan, R. Geospatial approach for assessing spatiotemporal dynamics of urban green space distribution among neighbourhoods: A Demonstration in Mumbai. *Urban For. Urban Green.* **2020**, *48*, 126585. [CrossRef]
32. Zhang, S.; Liu, J.; Song, C.; Chan, C.-S.; Pei, T.; Wenting, Y.; Xin, Z. Spatial-temporal distribution characteristics and evolution mechanism of urban parks in Beijing, China. *Urban For. Urban Green.* **2021**, *64*, 127265. [CrossRef]
33. Moussa, Y.M.; Diop, I.T.; Nassirou, I.; Nafiou, M.M.; Soulé, M. Determinants of the urban green spaces management practices in the city of Niamey, Niger. *Cities* **2024**, *144*, 104641. [CrossRef]
34. Wang, Y. The impact of economic growth target management on urban green land utilization efficiency. *PLoS ONE* **2025**, *20*, e0321779. [CrossRef] [PubMed]
35. Liu, W.; Li, H.X.; Xu, H.; Zhang, X.T.; Xie, Y.C. Spatiotemporal distribution and driving factors of regional green spaces during rapid urbanization in Nanjing Metropolitan Area, China. *Ecol. Indic.* **2023**, *148*, 110058. [CrossRef]
36. Ji, Y.W.; Zhang, L.; Li, C.T.; Gu, X.C. Investigating the drivers and mechanisms behind the spatial evolution of regional green spaces using geographically weighted regression: A case study of rapidly urbanizing regions. *Forests* **2026**, *17*, 585. [CrossRef]
37. Zang, Z.X.; Zhang, L.W.; Liu, Y.; Yang, X.P.; Wang, Z.Z.; Jiao, L.; Wang, H.; Luo, Y. A framework for analyzing spatial heterogeneity and influencing factors of campus green space in Xi'an, China. *Chin. Geogr. Sci.* **2025**, *35*, 786–801. [CrossRef]
38. Ouyang, L.P.; He, Y.C.; Chen, Z.F.; He, K. Dynamic monitoring and evolution of urban green space landscape sustainability based on spatiotemporal analysis algorithm. *Int. J. Environ. Sustain. Dev.* **2026**, *25*, 3–23. [CrossRef]
39. Wang, L.Y.; Wang, X. Toward equitable green spaces: Spatial patterns and determinants of accessibility and inequality across 314 Chinese cities. *Cities* **2026**, *173*, 106933. [CrossRef]
40. Cai, Z.H.; Zhao, S.D.; Huang, M.S.; Zhang, C.G. Evolution model, mechanism, and performance of urban park green areas in the grand canal of China. *Land* **2024**, *13*, 42. [CrossRef]
41. Zhao, S.; Zhang, P.; Li, W. A Study on Evaluation of Influencing Factors for Sustainable Development of Smart Construction Enterprises: Case Study from China. *Buildings* **2021**, *11*, 221. [CrossRef]
42. Yang, X.; Xu, J.; Zhao, S. Spatiotemporal dynamics and influencing factors of wood consumption in china's construction industry. *Buildings* **2025**, *15*, 917. [CrossRef]
43. Batasuma, S.; Cao, W.; Atigah, N.A.; Garnet, E.A.; Bonzo, J.K.; Gyimah, J. Drivers in the conservation of urban green space depletion: A case study of Wa Municipality, Ghana. *City Environ. Interact.* **2025**, *25*, 100186. [CrossRef]
44. Li, W.; Zhang, P.; Zhao, K.; Chen, H.; Zhao, S. The evolution model of and factors influencing digital villages: Evidence from Guangxi, China. *Agriculture* **2023**, *13*, 659. [CrossRef]
45. Li, W.; Wang, M.; Zhao, S. The Spatio-temporal dynamics, driving mechanism, and management strategies for international students in China under the Background of the Belt and Road Initiatives. *ISPRS Int. J. Geo-Inf.* **2023**, *12*, 405. [CrossRef]
46. Adorno, B.V.; Pereira, R.H.M.; Amaral, S. Combining spatial clustering and spatial regression models to understand distributional inequities in access to urban green spaces. *Landsc. Urban Plan.* **2025**, *256*, 105297. [CrossRef]
47. Zhang, P.; Li, W.; Zhao, K.; Zhao, S. Spatial pattern and driving mechanism of urban–rural income gap in Gansu province of China. *Land* **2021**, *10*, 1002. [CrossRef]
48. Zhao, S.; Li, W.; Zhao, K.; Zhang, P. Change characteristics and multilevel influencing factors of real estate inventory—Case studies from 35 Key Cities in China. *Land* **2021**, *10*, 928. [CrossRef]
49. Li, Z.Q. Extracting spatial effects from machine learning model using local interpretation method: An example of SHAP and XGBoost. *Comput. Environ. Urban Syst.* **2022**, *96*, 101845. [CrossRef]
50. Zhou, C.Y.; Wang, Z.; Wang, X.L.; Guo, R.; Zhang, Z.; Xiang, X.W.; Wu, Y.Q. Deciphering the Nonlinear and Synergistic Role of Building Energy Variables in Shaping Carbon Emissions: A LightGBM–SHAP Framework in Office Buildings. *Build. Environ.* **2024**, *266*, 112035. [CrossRef]
51. Ganjirad, M.; Delavar, M.R.; Bagheri, H.; Azizi, M.M. Optimizing urban critical green space development using machine learning. *Sustain. Cities Soc.* **2025**, *120*, 106158. [CrossRef]
52. Bille, R.A.; Jensen, K.E.; Buitenwerf, R. Global patterns in urban green space are strongly linked to human development and population density. *Urban For. Urban Green.* **2023**, *86*, 127980. [CrossRef]
53. Yang, M.X.; Zhu, L.; Hu, Z.G. Study on landscape pattern index analysis and driving mechanism of park green space: A case study of the central urban area of Shenyang. *Sustainability* **2026**, *18*, 4951. [CrossRef]

54. Rahaman, S.; Cai, D.M.; Cheng, Y.H.; Wei, X.; Gong, X.D. Ai-integrated framework for green space optimization and air quality improvement: A futuristic approach toward sustainable urban development. *Sustain. Cities Soc.* **2026**, *137*, 107117. [CrossRef]
55. Siddique, S.; Uddin, M.M. Green space dynamics in response to rapid urbanization: Patterns, transformations and topographic influence in Chattogram city, Bangladesh. *Land Use Policy* **2022**, *114*, 105974. [CrossRef]
56. You, Z.; Feng, Z.M.; Yang, Y.Z. Relief Degree of Land Surface Dataset of China (1 km). *J. Glob. Change Data Discov.* **2018**, *2*, 151–155. [CrossRef]
57. Exposito, A.; Espinosa, M.; Villa-Damas, A. Valuing visitor willingness to pay for urban green space conservation: Case of Maria Luisa Park in Seville, Spain. *J. Urban Plan. Dev.* **2021**, *147*, 05021020. [CrossRef]
58. Bressane, A.; Loureiro, A.I.S. Political and socioeconomic drivers of urban green space management: Insights from a case study in a Metropolitan Region of an Emerging Economy. *Urban For. Urban Green.* **2025**, *104*, 128591. [CrossRef]
59. Wang, T.W.; Du, X.F.; Feng, G.Q.; Hu, H.H. Hidden greens, hidden inequities? evaluating accessibility and spatial equity of non-park green spaces in London. *Sustainability* **2025**, *17*, 9284. [CrossRef]
60. Li, J.Y.; Yan, Y.W.; Stouffs, R. Reevaluating the equity of urban green space distribution: A proposed method integrating urban high-temperature hot spots and temporal dimensions. *Building Environ.* **2026**, *292*, 114274. [CrossRef]
61. Roodsari, E.N.; Hoseini, P. An Assessment of the correlation between urban green space supply and socio-economic disparities of Tehran Districts-Iran. *Environ. Dev. Sustain.* **2022**, *24*, 12867–12882. [CrossRef]
62. Zhang, G.S.; Su, Y.; Wang, Z.M.; Chen, Y.; Wan, J.J.; Bai, H.C. Spatial-temporal evolution and driving force analysis of blue-green space in the Chengdu-Chongqing Economic Circle, China. *Land* **2024**, *13*, 1733. [CrossRef]
63. Yang, H.; Jin, C.; Li, T. Megacity urban green space equity evaluation and its driving factors from supply and demand perspective: A case study of Tianjin. *J. Clean. Prod.* **2024**, *474*, 143583. [CrossRef]
64. Wang, H.M.; Lin, C.R.; Ou, S.H.; Feng, Q.Y.; Guo, K.; Xie, J.Z.; Wei, X.J. Evolutionary characteristics and driving forces of green space in Guangzhou from a Zoning Perspective. *Forests* **2024**, *15*, 135. [CrossRef]
65. Li, X.; Ma, X.D.; Hu, Z.N.; Li, S.Y. Investigation of urban green space equity at the city level and relevant strategies for improving the provisioning in China. *Land Use Policy* **2021**, *101*, 105144. [CrossRef]
66. Huang, Y.H.; Wang, L.H.; Yang, L.; Mapfumo, P.; Irandu, E.M.; Du, Y.; Ling, F. Drivers and dynamics of urban green spaces in Africa: A remote sensing perspective in the 21st century (2000–2024). *Urban For. Urban Green.* **2026**, *118*, 129244. [CrossRef]
67. Kasahun, M.; Diriba, D.; Engdaw, G.; Karuppannan, S.; Shewaye, G. Geospatial multi-criteria analysis for urban green space suitability and expansion planning in nekemte town, Ethiopia. *Discov. Sustain.* **2025**, *7*, 139. [CrossRef]
68. Wei, L.; Liu, Z.H.; Zhou, Y.; Tao, Z.W.; Yang, F. Global urban green spaces in the functional urban areas: Spatial pattern, drivers and size hierarchy. *Urban For. Urban Green.* **2025**, *107*, 128770. [CrossRef]
69. Liu, M.; Li, J.X.; Song, D.; Dong, J.M.; Ren, D.J.; Wei, X.Y. Spatiotemporal dynamics effects of green space and socioeconomic factors on urban agglomeration in Central Yunnan. *Forests* **2024**, *15*, 1598. [CrossRef]
70. Chang, J.F.; Wang, W.; Liu, J.L. Industrial Upgrading and Its Influence on Green Land Use Efficiency. *Sci. Rep.* **2023**, *13*, 2813. [CrossRef] [PubMed]
71. Liu, X.; Li, Y.; Xi, H.; Li, X.; Wu, Y.; Yuan, S.; Xu, M.; Ou, W.; Huang, C. Assessing spatial pattern of urban green space coverage and its determining factors: A case study in the Yangtze River Delta region in China. *Adv. Space Res.* **2025**, *75*, 3362–3374. [CrossRef]
72. Shi, T.L.; Xu, H. Study on ecosystem service values of urban green space systems in Suzhou city based on the extreme gradient boosting geographically weighted regression method: Spatiotemporal changes, driving factors, and influencing mechanisms. *Land* **2025**, *14*, 564. [CrossRef]
73. Wang, J.N.; Wang, W.C.; Zhang, S.S.; Wang, Y.Y.; Sun, Z.H.; Wu, B.L. Spatial and temporal changes and development predictions of urban green spaces in Jinan City, Shandong, China. *Ecol. Indic.* **2023**, *152*, 110373. [CrossRef]
74. Li, Y.Z.; Yu, D.B.; Zhang, X.D. The spatiotemporal evolution and impact of green land use efficiency in resource-based cities in the yellow river basin under the background of sustainable development. *Front. Environ. Sci.* **2024**, *12*, 1406460. [CrossRef]
75. Doan, Q.C. The spatiotemporal trends of urban-rural green spaces and their heterogeneous relationships with population and economic vitality: Evidence from the Red River Delta, Vietnam. *Socio-Econ. Plan. Sci.* **2024**, *93*, 101885. [CrossRef]
76. Nor, A.N.M.; Aziz, H.A.; Nawawi, S.A.; Jamil, R.M.; Abas, M.A.; Hambali, K.A.; Yusoff, A.H.; Ibrahim, N.; Rafaai, N.H.; Corstanje, R.; et al. Evolution of green space under rapid urban expansion in southeast Asian cities. *Sustainability* **2021**, *13*, 12024. [CrossRef]
77. Wu, C.; Yang, S.; Ma, Y.B.; Liu, P.Y.; Ye, X.Y. Urban green space assessment: Spatial clustering method based on multisource data to facilitate zoning planning. *J. Urban Plan. Dev.* **2024**, *150*, 04024032. [CrossRef]
78. Li, X.M.; Zhang, D.Y.; Yang, Y.; Li, W.W.; Nan, X.Y.; Zhao, T.R.; Yan, F.; Bao, G.L. Drivers of urban blue-green space loss: A study on the coordination between economic growth and land use change. *Front. Environ. Sci.* **2026**, *14*, 1774328. [CrossRef]
79. Zhang, J.F.; Chen, Y. Aligning objective provision and lived experience: A dual-model assessment of urban park equity and efficiency in chengdu's "Park City" initiative. *Urban For. Urban Green.* **2026**, *120*, 129438. [CrossRef]

80. Liu, B.X.; Tian, Y.; Guo, M.; Tran, D.; Alwah, A.A.Q.; Xu, D.W. Evaluating the disparity between supply and demand of park green space using a multi-dimensional spatial equity evaluation framework. *Cities* **2022**, *121*, 103484. [CrossRef]
81. Wu, S.Z.; Wang, D.Y.; Yan, Z.R.; Wang, X.J.; Han, J.Q. Spatiotemporal dynamics of urban green space in Changchun: Changes, transformations, landscape patterns, and drivers. *Ecol. Indic.* **2023**, *147*, 109958. [CrossRef]
82. Aduloju, O.T.; Anofi, A.O.; Chukwu, M.T.; Adeniran, I.A.; Adekunle, S.T. Space-time analysis of urban green spaces' disappearance in Ilorin, Nigeria. *Prof. Geogr.* **2025**, *77*, 169–185. [CrossRef]
83. Zhao, K.X.; Chen, C.; Wang, J.M.; Liu, K.X.; Wu, F.Q.; Cao, X.T. Examining the spatial mode, supply-demand relationship, and driving mechanism of urban park green space: A case study from China. *Forests* **2024**, *15*, 131. [CrossRef]
84. Zhang, Z.X.; Du, S.J.; Qian, L.; Qian, G.Y.; Shi, Z.W.; Yan, C. Analysis of spatial and temporal characteristics and influence mechanisms of blue-green spaces in China's, 2000-2020. *Ecol. Indic.* **2025**, *178*, 113903. [CrossRef]
85. Wu, W.L.; Yuan, Y.; Huang, C.B.; Dong, W.; Fu, Z.C. Urban green land ecological suitability assessment based on GIS in arid areas: Beitun City, Xinjiang, as an Example. *Pol. J. Environ. Stud.* **2022**, *30*, 5871–5883. [CrossRef]
86. Zhu, J.J.; Jiang, Y.; Wang, C. From spatial mismatch to urban equity: A governance-oriented supply-demand coupling framework for evaluating urban park green space equity in high-density Tianjin. *Int. J. Urban Sci.* **2026**, 1–36. [CrossRef]
87. Farkas, J.Z.; Hoyk, E.; de Morais, M.B.; Csomos, G. A systematic review of urban green space research over the last 30 years: A bibliometric analysis. *Heliyon* **2023**, *9*, e13406. [CrossRef] [PubMed]

Disclaimer/Publisher's Note: The statements, opinions and data contained in all publications are solely those of the individual author(s) and contributor(s) and not of MDPI and/or the editor(s). MDPI and/or the editor(s) disclaim responsibility for any injury to people or property resulting from any ideas, methods, instructions or products referred to in the content.